# Adhesion loss at epoxy/glass interfaces under hygrothermal conditions.

# ADHESION LOSS AT EPOXY/GLASS INTERFACES UNDER HYGROTHERMAL CONDITIONS

by

**Xiaohan Zhang**

**A Dissertation**

**Presented to the Graduate and Research Committee**

**of Lehigh University**

**in Candidacy for the Degree of**

**Doctor of Philosophy**

**in**

**Polymer Science and Engineering**

**Lehigh University**

**2006**

# Certificate of Approval

Approved and recommended for acceptance as a dissertation in partial fulfillment of the requirements for the degree of Doctor of Philosophy.

12/5/2006
Date

Dr. Raymond A. Pearson
Dissertation Advisor

12/5/2006
Accepted date

Special committee directing the
Doctoral work of Xiaohan Zhang

Dr. Raymond A. Pearson, Chairperson

Dr. Miltiadis K. Hatalis

Dr. Herman F. Nied

Dr. Donna Narsavage-Heald

Dr. Don Herr

# Dedication

To my dear teachers, family and friends

# Acknowledgement

First of all, I would like to express my sincere gratitude to my advisor Prof. Pearson for his guidance, patience and constant encouragement over the years. I can not imagine a better advisor.

I appreciate the time and effort spent by my committee members, Prof. Hatalis, Prof. Nied, Prof. Donna Narsavage-Heald and Dr. Don Herr. Their valuable discussions, suggestions and guidance offered great help on this research project.

I would also like to express my gratitude to Prof. Sperling for the discussions, help and great support received from him.

I am grateful to the research scientists and engineers in the Materials Sci. & Eng. Dept. and COT: Dave Ackland, Arlan Benscoter, Gene Kozma, Alfred Miller, William Mushock, Michael Rex. Their support made my research carried on smoothly.

I want to thank everyone in our microelectronic packaging group, Steve Antalics, Brian McAdams, Peerapan Dittanet, Ryan Hydro, Robert Oldak, Yilin Liang, Seymour Pries, Pat Hoontrakul, Orasa Khayankarn, Guy Connelly, Jeff Shakespeare and Jason Iceman.

Finally, I want to thank my family and friends. Their support and love make everything possible for me.

# Table of Contents

# LIST OF TABLES

# LIST OF FIGURES

# Abstract

The adhesion loss at epoxy/glass interfaces under hygrothermal conditions was investigated. One thermal cured model epoxy system and one UV cured developmental epoxy system were used in this study. Several factors that could affect the adhesive strength of the epoxy/glass joints were evaluated to get a better understanding of adhesion loss of adhesive joints under hygrothermal conditions. A model was proposed to predict/calculate the adhesion loss at the epoxy/glass interface for this experimental adhesive.

The effect of surface treatment of the substrate on adhesion loss was studies. Two coating procedures were used: 1) a monosilane and dipodal mixture, or 2) dipodal-then-monosilane two-step process. The results were compared with the adhesion strength by a monosilane treatment. It was found that the mixture of dipodal silane coupling agent and monosilane resulted in poor adhesion between epoxy and glass substrate.

For a two-step treatment, BTSE and GPS are selected for the investigation and it offers better moisture resistance for the model epoxy systems than bare glass surface or GPS treated glass surface. The rate of adhesion loss of those adhesive joints is slower than GPS treated surface or bare glass. However, for a longer time, when the adhesion drops to a plateau region, the adhesive joint by two-step treatment does not show significantly

better adhesion than GPS treated surface or the bare glass surface.

XPS is used to investigate the locus of failure. It was found that the failure mode for BTSE/GPS coated surface is cohesive failure when the specimen is dry. The fracture surface is within epoxy bulk. After hygrothermal aging, the failure mode is adhesive failure.

A model is proposed to predict adhesion loss based on the area of cohesive failure and adhesive failure on a commercial UV cured epoxy. The predicted values of adhesion by the model fit well with the experimental data. SEM is used to obtain the images of fracture surfaces.

# CHAPTER 1

# INTRODUCTION

---

## 1.1 Current status of OLED/PLED on flexible display applications

Organic Light Emitting Diodes (OLEDs) include both small-molecular and polymer-based devices, which are known as a promising display technology nowadays. The first OLED based was fabricated in 1963 [1], In 1990 Friend et al. of Cambridge University described the first polymer OLED (PLED) based on the conjugated polymer polyparaphenylenevinylene (PPV) which was a single-layer device structure [2]. The inherent thin-film structure of OLED/PLED makes them attractive for flexible displays, which is one of the hottest topics in the flat panel display industry. In the past decade advances in OLEDs technology make the future of flexible displays very promising. Compared to traditional displays, OLEDs have many advantages such as high brightness and contrast ratio, low operating voltages, low manufacture cost,

wide viewing angle, fast response time and low energy consumption. They can be used on cameras, cell phones, watches, PDAs, computer monitors, TV screens and a lot more applications. It is also promising to use them as electronic news paper or retractable PDAs.

Improvement of device fabrication and stability of OLED/PLED devices in recent years made the commercialization of OLED possible. Many companies, including Toshiba, Sony, Creative and Samsung, have applied OLED and PLED on commercial products such as GPS, MP3 players, cell phones, car radios, etc. They are beginning to replace LCDs in handheld devices. In 2005, Samsung introduced their prototype product of 40 inch OLED TV, which has 1:1000 contrast ratio, and only 12mm thick. But it is not ready for commercialization yet. The current commercially available products, such as digital cameras or cell phones, require relatively short life time and operating time of the displays. Degradation of the light emitting layer still limits them to be applied on monitors or televisions. The light emitting layer in the display is extremely sensitive to oxygen and water. It will easily degradate and lose its luminescence. [5].

One solution for this problem is to encapsulate the display in an inert atmosphere. The display can be protected by using glass on top and encapsulating by proper sealant. In such case, the properties of the sealant are

crucial. Especially when used in hot and humid environment, the ability of the sealant to resistant water and oxygen would determine the lifetime of the products. When the products are used in Singapore, the lifetime could be much shorter than used in Canada due to higher humidity and temperature.

## 1.2 Diffusion Coefficient

One important parameter for water resistance is diffusion coefficient. According to Fick's second law with a constant diffusion coefficient of diffusivity, D [6] is

$$\frac{\partial c}{\partial t} = D\nabla^2 c \tag{1.1}$$

where c is moisture concentration t is time. For one dimensional diffusion through an infinite plate of thickness L, it can be expressed as [7]:

$$\frac{\partial c}{\partial t} = D_x \frac{\partial^2 c}{\partial x^2} \tag{1.2}$$

where Dx is the diffusivity through the thickness of the material. The

diffusion of moisture into glassy polymers generally follows this law when this moisture transport is completely controlled by concentration gradients, and when degradation, molecular relaxation, or insufficient curing are not active [8].

Dx is dependent on temperature following an Arrhenius relationship [9] by:

$$D_x = D_0 \exp\left(\frac{-\Delta H}{RT}\right) \tag{1.3}$$

where

D is the diffusion coefficient ($m^2s^{-1}$)

$D_0$ is the maximum diffusion coefficient (at infinite temperature) (K)

$E_A$ is the activation energy for diffusion ($J\ mol^{-1}$)

T is the temperature (K)

R is the gas constant ($J\ K^{-1}\ mol^{-1}$)

## 1. 3 Epoxy adhesives

Epoxy adhesives have good bonding to all kinds of substrates at dry condition. Compared to other polymeric adhesives, they have less adhesion

loss under wet condition. Often used as encapsulants, epoxies also have excellent resistance to water absorption and permeation. For electronic grade epoxies, equilibrium water absorption values are from 0.1% to 0.25%. Epoxies have very low shrinkage rate in comparison to other adhesives. The volumetric shrinkage of epoxies is typically less than 4%. Lower shrinkage greatly reduces residual stress, and the tendency to crack, which result in increased stability. [10]

In recent years, UV-cured epoxies have shown their advantages in coating, adhesive and sealant applications. Typical epoxies fro these applications used to be thermal cured, or air-dry ambient cured. Such curing methods have distinct disadvantages. Thermally cured systems require high temperature, which consumes more energy, and also could be harmful to the parts to be encapsulated. The air-dry ambient cured systems may involve solvents, and take longer to cure. The UV cured epoxies were developed to address these problems. Such epoxies contain special oligomers, monomers and photo-initiators. UV light is used to initiate the crosslinking reaction. Therefore, UV-cured systems have several advantages over heat or ambient cured epoxies. They consume less energy, can be cured at room temperature, need less space for curing, and can be cured in seconds.

All of the above properties make epoxies, especially UV-cured epoxies

good candidates as sealants for OLED/PLED displays.

## 1. 4 References


1. M. Pope, H. Kallmann, and P. Magnante, "Electroluminescence in organic crystals," J. Chem. Phys. 38, 2042 (1963).
2. J. H. Burroughes, D. D. C. Bradley, A. R. Brown, R. N. Marks, K. MacKay, R. H. Friend, P. L. Burn, and A. B. Holmes, Nature 347, 539 (1990).
3. P. E. Burrows, G. Gu, V. Bulovic, Z. Shen, S. R. Forrest, and M. E. Thosmpson, "Achieving full-color organic light-emitting devices for light weight, flat-panel displays," IEEE T. Electron Dev., vol 44, pp 1183-1203, (1997).
4. Z. Shen, P. E. Burrows, V. Bulovic, S. R. Forrest, and M. E. Thompson, "Three-color, tunable, organic light-emitting devices," Science, vol.276, pp. 2009-2011, (1997).
5. M. S. Xu, J. B. Xu, H. Z. Chen and M. Wang, J. Phys. D: Appl. Phys. 37, 2618, (2004).
6. T. Alfrey, E. F. Gurnee, and W. G. Lloyd, Journal of Polymer Science, Part A: Polymer Chemistry, 1, 249, (1966).
7. C. E. Browning, G. E. Husman, and J. M. Whitney. in Composite Materials: Testing and Design, ASTM STP 617, American Society for

Testing and Materials. Philadelphia, PA. (1977).

8. J. M. Whitney, C. E. Browning, in Advanced Composite Materials-Environmental Effects, ASTM STP 658, American Society for Testing and Materials. Philadelphia, PA. (1978).
9. C. H. Shen, and G. S. Springer, Journal of Composite Materials, 10: p. 2, (1976).
10. C. A. May, Epoxy resins, chemistry and technology, 2nd edition,(1988).

# CHAPTER 2

# BACKGROUND

## 2.1 Overview of Adhesives

Adhesives have been used for thousands of years. In modern industry and everyday life, the use of adhesives is everywhere. The primary boost of the use of adhesives was accompanied with the advent of synthetic polymeric materials with improved properties [1].

Adhesives joints do not exhibit high stress concentrations when properly designed. Fatigue failures are generally delayed compared to mechanical fastening. Shock-sensitive materials used in adhesive joints are less likely to fail than those used in mechanical fastening [1]. These advantages make adhesives widely used in aerospace industry. Intensive studies on adhesion promoters have been performed for aerospace industry in order to improve adhesion between adhesives and substrates [2,3, 4, 5].

The disadvantages of adhesive joints are that they depend strongly on the character of the surface of the adherend and how the adhesive interacts with the surface. Surface problems could be even more important in severe environments [6]. Many adhesives lose adhesion when exposed to hot, humid environments as shown in Figure 2.1 [7]. The fracture stress of butt joints decreases with increasing temperature with the presence of water. The higher temperature, the faster the drop of fracture stress.

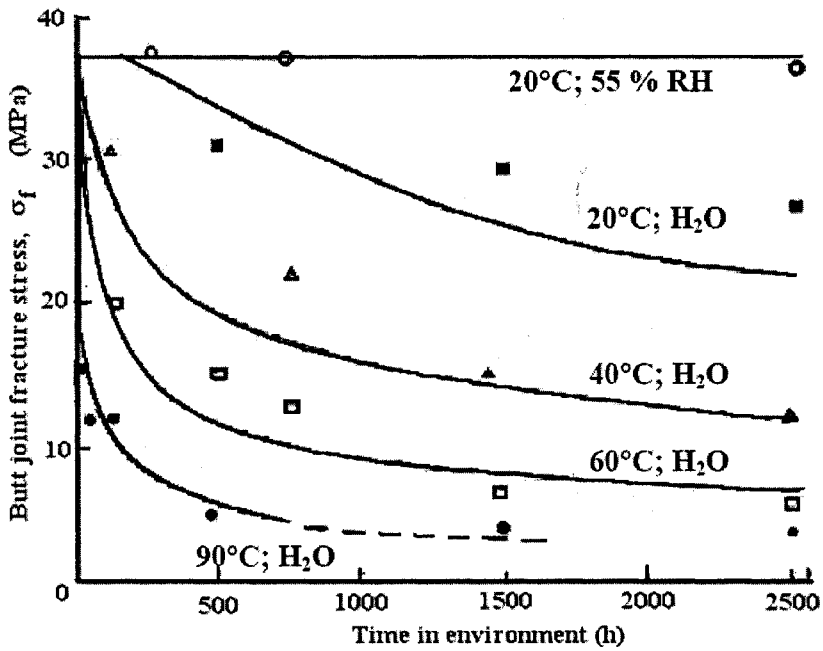


***Figure 2.1*** *Adhesion loss under hygrothermal aging [7]*

## 2.2 Mechanical tests of adhesive joints

There are three types of forces that can be applied to an adhesive. They are tension, shear and cleavage, as seen in Fig. 2.2. There are three possible fracture modes when a fracture is initiated in a cracked adhesive joint: mode I (cleavage), mode II (shear) and mode III (tearing), as seen in Figure 2.3. The most common mode is mode I. Table 2.1 lists and briefly describes various ASTM testing methods of adhesive bonds [1]. Among those tests, Double Cantilever Beam (DCB) test is being used for determining the Mode I fracture toughness. Strain energy release rate can be obtained by DCB or ADCB tests. Matthew et al. [8] showed that for an elastic body, the strain energy release rate is related to the compliance (displacement/load)

## 2.3 Measurement of adhesion strength

Griffith is often cited as a major contributor to the birth of fracture mechanics. In fracture mechanics, it is assumed that all real "elastic" bodies have inherent flaws in them. A quantity of energy is needed to make the most critical of these cracks grow would need to come from the strain energy in the body and work applied by loads. The mechanical strength or toughness of an interface has essentially two components: the energy required to separate the two adjoining materials to create two new free surfaces, and energy used to overcome the deformation of the materials at the crack tip and surrounding

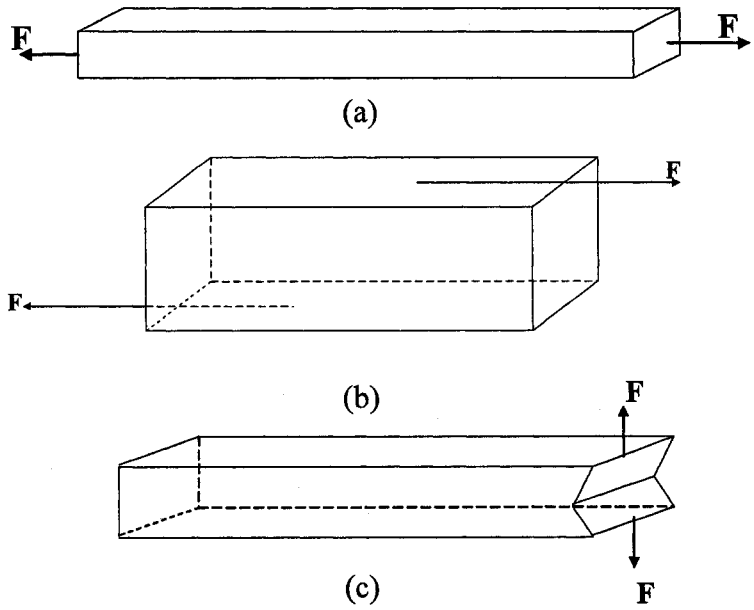


***Figure 2.2*** *Three types of forces applied to adhesives (a) tensile (b) Shear (c) Cleavage*

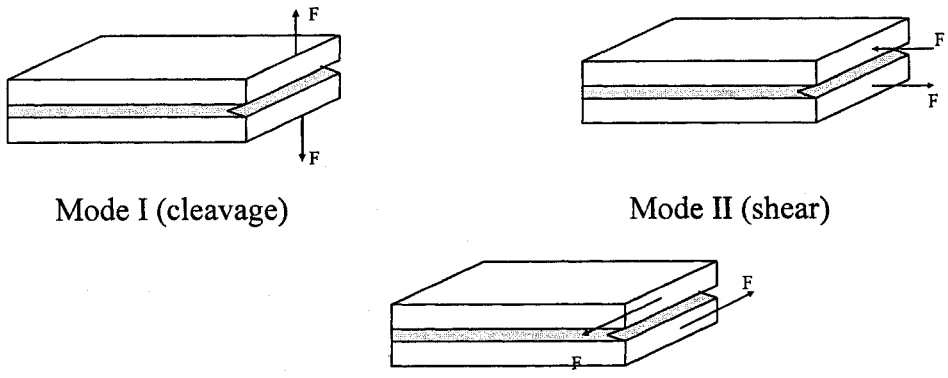


***Figure 2.3*** *Schematic of the three modes of fracture. Mode I is know as cleavage, Mode III know as shearing. Mode III is known as tearing.*

area during the advancing of interface crack. It is typically quantified in terms of a critical energy release rate for crack extension along the interface (Gc), measured in units of energy per unit area [9].

The energy consumed in creating two new free surfaces can be characterized in terms of surface tensions of these two surfaces. Contact angle measurements can be used to characterize the thermodynamic work of adhesion by the following equation [9, 10]:

$$W_{12} = \gamma_1 + \gamma_2 + \gamma_{12} \tag{2.1}$$

where $W_{12}$ is the thermodynamic work of adhesion (Helmholtz free energy per unit area), $\gamma_1$ is the surface tension of substrate 1, $\gamma_2$ is the surface tension of substrate 2, and $\gamma_{12}$ denotes the interfacial surface energy of these two materials.

In a perfect elastic system where excessive plastic deformation is absent from both materials, it is convenient to relate surface free energies to a critical strain energy release rate, $G_C$:

$$G_C = W_{12} = 2\gamma_1. \tag{2.2}$$

Griffith hypothesized that all real "elastic" bodies have inherent cracks in them and that a quantity of energy to make the most critical of these cracks grow would need to come from the strain energy in the body and work applied by loads. Conservation of energy dictates that a crack can grow only when the strain energy released as the crack grows is enough for the energy required to create the new "fracture" surface. When a crack propagates, a critical strain energy release rate, $G_C$, is defined as follows:

$$G_C = \frac{1}{B}\frac{dU}{da} \tag{2.3}$$

For a system that viscoelastic or plastic processes can not be ignored, there will be an extra term to count viscoelastic losses at the crack tips:

$$G_C = W_{12}(1+\phi) \tag{2.4}$$

where $\phi$ is a term related to the energy loss other than the thermodynamic work of adhesion. In fact, the energy dissipated by other means often dominates the process and may be several orders of magnitude higher than the chemical surface energy ($\phi >> 1$). However, that does not indicate that Equation 2.4 is definitely not suitable for the case where the material involved is not ideal elastic. As explained in modern texts on fracture

mechanics, this Equation (2.4) can still be used for analysis of fracture in quasi-elastic systems. The energy consumed by other dissipation mechanisms assume also follows that relationship and can simply be included into the fracture energy term $G_C$.

Although fracture mechanics was originally developed for bulk materials [13], it can be applied to failure of the interface between two materials. The various sample geometries employed and analysis of experiments are directly analogous to those used in fracture tests for bulk materials. Instead of testing a large, continuous piece of material, one sandwiches the interface that is to be debonded between two relatively thick "beams". The interface is debonded by applying loads to the beams. The beams bend in response to the loads, building up elastic strain energy. When the interface between the beams debonds, some of the strain energy is relaxed, and it is this relaxation energy that provides a driving force for debonding.

These "beam bending" techniques have many advantages. The quantity that is being measured, the energy required to delaminate an interface, is well defined. The techniques are amenable to the study of low velocity, environmentally-influenced debond growth and to debond growth under fatigue loads. Thick beams are described quite accurately by a simple linear-elastic model, and the technique does not rely upon storing large amounts of

strain energy in a thinly layered material. Results are not unduly influenced by quantities such as residual stress of the material that is debonding. In practice, one can obtain repeatable measurements with low scatter.

Among various test specimens that have been used to measure the critical strain energy release rate, $G_C$, the Double Cantilever Beam (DCB) specimen, shown in Figure 2.4, is one of the most popular methods.

In the double cantilever configuration, the ends of the sample are pulled apart, forcing a crack to propagate down the beam from one end. Loads are applied to the sample through metal tabs epoxied to the beams. During the test we measure the force applied through the loading tabs and the displacement of the beam ends. The length of the interface crack may be obtained optically from observation with a microscope, or can be inferred from measurements of the sample's compliance. From simple beam theory, the energy release rate, $G_C$, for DCB samples is approximately:

$$G_C = \frac{12P^2a^2}{B^2h^3E_s} \tag{2.5}$$

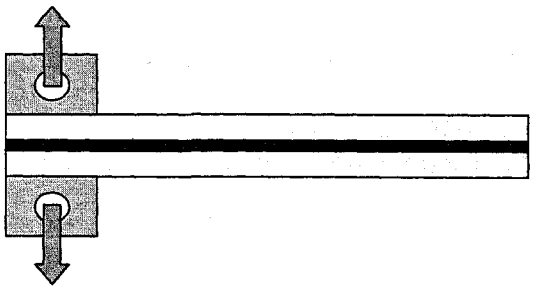

***Figure 2.4*** *A Double Cantilever Beam Sample*

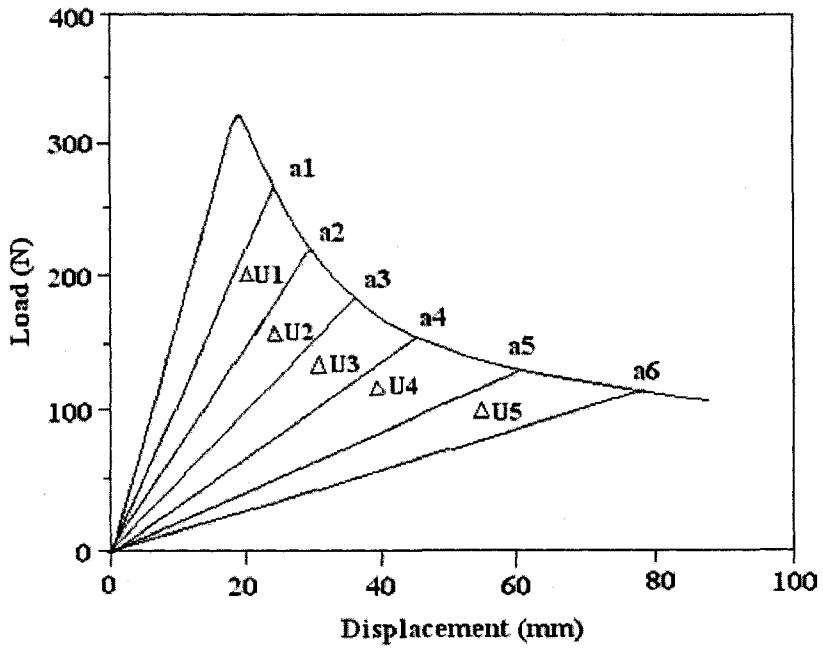


***Figure 2.5*** *Schematic drawing of a DCB curve*

Fig. 2.5 shows a schematic drawing of a DCB loading-unloading curve.

## 2.4 Organosilane-based adhesion promoter

### 2.4.1 Definition

Organofuncitional silanes may be used as adhesion promoters between organic polymer and mineral substrates under a variety of circumstances [2]. The silane adhesion promter, or "coupling agent", may form chemical bonding at both organic and inorganic surfaces to obtain better adhesion.

Organosilane-based adhesion promoters have multiple functional groups that can react with or affiliate to inorganic materials, and others may react with or affiliate to organic materials. Thus they have the ability to form durable bonds between organic and inorganic materials. This property makes many organosilanes-based adhesion promoters extremely used and they have been widely used and studied [2].

**Table 2.1** Selected ASTM test methods pertaining to the determination of cleavage or shear properties of adhesive bonds

| Test | Title of test | Short description of test |
|---|---|---|
| D903 | Test method for peel or stripping strength of adhesive bonds | A thin adherend is bonded to a thick adherend. The thin adherend is stripped from the thick one at a 180° angle. |
| D1062 | Test method for cleavage strength of metal-to-metal adhesive bonds | Blocks of metals are bonded together and the specimen is loaded to make a cleavage load on the adhesive. Different from D903 in that neither adherend is flexible. |
| D1781 | Practice for climbing drum peel test for adhesives | A test method used primarily in the aerospace industry in which a thin adherend is stripped from a thicker adherend by having a drum "climb" the bond. Also used to measure the stripping force to remove a face sheet from a honeycomb sandwich bond. |
| D1876 | Test method for peel resistance of adhesives (T-peel test) | The most widely used peel test in which two equally thick, flexible adherends are bonded together and then peeled apart in a symmetrical fashion such that the bond looks like a "T" while peeling. |
| D3433 | Practice for fracture strength in cleavage of adhesives in bonded joints | A double cantilever beam test used to measure $G_C$ for adhesives. Thick adherends are used. |
| D3762 | Test method for adhesive bonded surface durability of aluminum (wedge test) | A think adherend fracture test in which surface-prepared metal is adhesively bonded and then a wedge is driven into the edge of the bond. The bond is exposed to a adverse environment and crack growth is measured. |
| D3807 | Test method for strength properties of adhesives in cleavage peel by tension loading (plastic-to-plastic) | A cross between D3433 and D1876 in which thick plastic samples are bonded and then pulled apart in mode similar to that of D3433. |
| D5041 | Test method for fracture strength in cleavage of adhesives in bonded joints | Thick adherends are bonded together with a bead of adhesive that is remote from the end of the test specimen. A specified wedge is driven into the end of the specimen and the energy to propagate a crack is measured . |

The general structure for a typical organosilane coupling agent shows the two classes of functionality. X is a hydrolyzable group typically alkoxy, acyloxy, halogen or amine. After hydrolysis, a reactive silanol group is formed, that can react with other silanol groups through a condensation reaction. For example, those organosilanes can covalently bond to the surface of the substrate, to form siloxane linkages. The R group is a nonhydrolyzable organic group that has a wide range of possibility selections. It is common to select a functionality that desired to react or interact strongly with polymeric material.

Most of the widely used organosilanes have one organic groups linked to silicon atom and three hydrolyzable groups as shown in Fig. 2.6. Most often, trialkoxysilanes are used. Reaction of these silanes involves four steps. Initially, hydrolysis of the three alkoxy groups occurs. Then, these hydrolyzed silanes condense to form oligomers. The oligomers then form hydrogen bonds with OH groups of the substrate. Finally during drying or curing, a covalent linkage is formed with the substrate and loss of water molecules. These reactions can occur simultaneously after the initial hydrolysis of one of the three alkoxy groups. At the interface, there is usually only one bond from each silicon of the organosilane to the substrate surface. The two remaining silanol groups are present either in free form or condensed with another hydrolyzed silane molecules. The R group remains available for covalent reaction or

physical interaction with the surfaces of organic material.

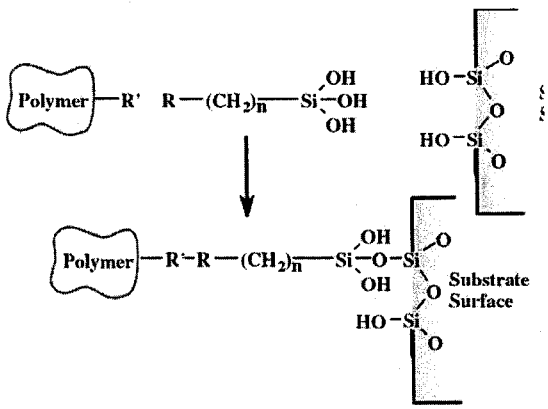


***Figure 2.6*** *Silane forming chemical bond between polymer and inorganic substrate*

### 2.4.2 Mechanism of Bonding of Organosilane -based Adhesion Promoter

Many theories about the mechanism of adhesion promoters have been described [14], but it is likely that more than one mechanism can be applied on the coupling agents in general. The mechanisms described below are the ones that have been widely accepted.

- Chemical Bond Theory

  According to this theory, trialkoxysilane groups chemically bond to silanols on the substrate surface by the reaction of hydrolyzed alkoxy

groups forming interfacial bonds; the organofunctional groups bond chemically to the polymer molecules [15, 16, 17, 18, 19].

Many studies have been undertaken to detect the chemical bonding of organosilanes with various surfaces. Miller and Ishida used infrared spectroscopy (IR) spectrum to find out that on the interaction of silanes on lead oxide surfaces and showed the formation of Pb-O-Si exhibiting an antisymmetric stretching vibration [32]. Schmidbaur also had similar findings [33, 34]. Boerio and Gosselin found Si-O-Al bonds and Si-O-Si asymmetric stretching vibration and low molecular weight oligmoers when studying the adsorption of APS onto aluminum substrates [35, 36].

Brindle et al. reported the interaction of silanes with silica gel by using solid state NMR [37]. Bauer et al. also reported their work on the characterization of silane modified silica particles using NMR [38].

A variation of the standard XPS method has been used by Mitchell's group at the University of British Columbia to study silane interfacial chemistry to study the deposition of silane on metal interfaces [39, 40].

Williams [32], and Gettings and Kinloch [42] reported to use SIMS to detect the interfacial bond of Fe-O-Si. Abel et al. [4] also used ToF-

SIMS to obtain evidence of the covalent bond formed between GPS and aluminum.

Shown in Fig. 2.7, the fragment Al-O-Si+ is in the spectrum and is sufficient to establish that interfacial covalent bonding exists [4]. It was also accompanied by the fact that the strength of the wedge joints was improved by applying GPS on aluminum.

Kent et al. [54] used self assembly monolayers to study the interaction between silane and adhesives. As seen in Figure 2.8. Increasing the percent of bromine terminated silane adhesion promoter increases adhesion strength ($G_C$). A linear variation in interfacial toughness with the percent of bromine-terminated chains, which forms a self-assembled monolayer.

- Acid-Base Reactions

Metal oxides have different isoelectric points in water and may therefore be regarded as acidic or basic, addition of materials having acidic properties to adhesives to be used on basic substrates, or basic materials for use on acidic substrates, may improve adhesion [20]. Acid-base reactivity

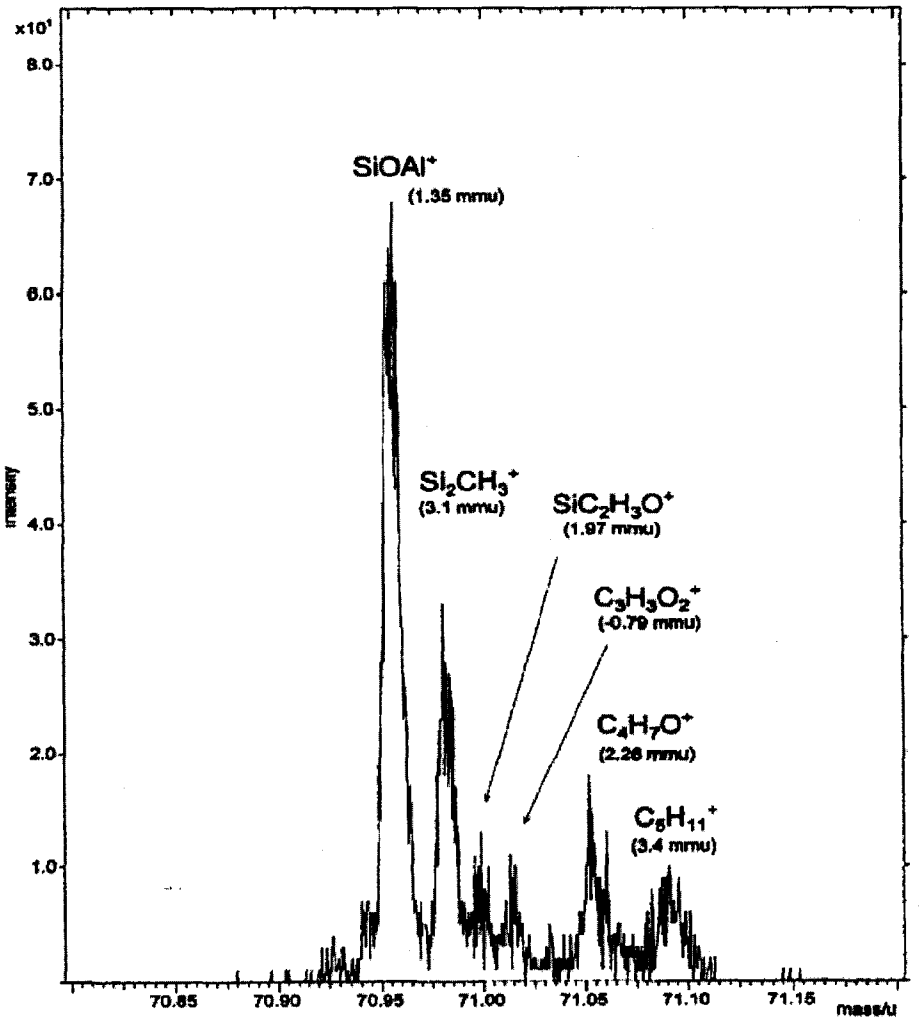


***Figure 2.7*** *High resolution mass spectrum of GPS coated aluminum in the mass range of m/z=70.9 to 71.15 Daltons. [4]*

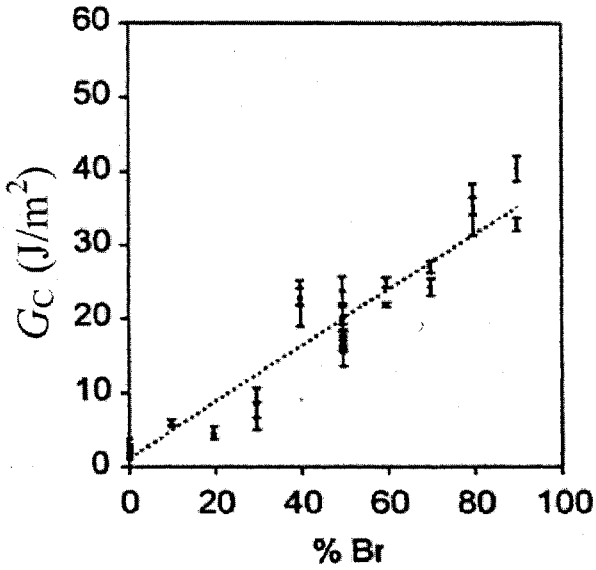


***Figure 2.8*** *Variation of GC with the % of bromine termination in the mixed monolayer SAM coating [54]*

reactions may also be important in aligning silane coupling agents on a filler surface [21].

- Other theories include:

  Deformable layer theory: postulates that interfacial layer can reduce internal stress by plastically deformation [14, 20].

  Restrained Layer Theory: proposed that the resin in the region of mineral filler should have a modulus somewhere between that of the mineral and the matrix resin, and suggests that the silane "tightens up" the

polymer structure in the interphase region [23, 24].

Tough Composites from Rigid Resins: The structure of silane on mineral substrate, elastomeric interlayer, and rigid matrix resin provides improved toughness while retaining good adhesion and water resistance [26].

Surface Wettability Theory: suggests that complete wetting of the mineral surface will improve adhesion by physical adsorption that would exceed the cohesive strength of the polymer. [15].

Many parameters affect the polymeric-inorganic bonding with silane adhesion promoter. These theories may explain one or more factors involved in improving the bonding using organosilane adhesion promoter.

Reversible Hydrolytic Bond Theory: argues that when the substrate bonds are broken by water ingress, they may re-form with some recovery in adhesion. It is likely that hydrogen bonding is a particularly important aspect of this theory, especially in the case of silanes [26]. Recovery of adhesion between urethane and epoxide coatings and metal substrates on drying out after water immersion was proved [27, 28, 29]. Some silane coupling agents do not need to react with the polymer chemically to

provide enhanced initial and wet adhesion [30].

### 2.4.3 Overview of organosilane adhesion prmoters

#### *2.4.3.1 Choice of organosilanes*

Many types of adhesion promoters are effective with epoxy resins, but when choosing from them, certain generalizations can be applied to get the optimum properties for the certain epoxy system. The silane coupling agent should have reactivity at least comparable to the epoxy systems. The glycidoxypropyl silane is an obvious choice for the epoxy systems, and cycloaliphatic silane is recommended with cycloaliphatic epoxides or with any epoxy using an acid or anhydride cure. APS can be used with the epoxy systems with amine curing agents. [1]

#### *2.4.3.2 Processing parameters*

In aerospace industry, metal pretreatment used to consist of phosphating and/or chromating, which are inexpensive and effective, but toxic and carcinogenic. Silane coupling agents can be used as an alternative choice for metal pretreatment. Silane treatment is an alternative method to replace toxic chemicals [43, 44, 45, 46]. It is worth mentioning that "international collaborative program on organosilane adhesion promoters" (ICOSAP), involving in scientists from the US and Europe, has developed detailed

understanding of the relationships between silane application variables, solution and surface chemistry, joint durability and mechanisms of failure. [47, 48] They have performed a detailed of a lot of investigation of GPS on aluminum surfaces. The findings are currently used for aerospace repair purposes.

Processing parameters such as temperature of cure, aging time, and concentration of the adhesion promoter solutions have been evaluated. A review of those studies offers a good guide in our determining processing parameters in this project.

- Temperature

  Surface analysis techniques such as ToF-SIMS and XPS were used to study the curing temperature of silane adhesion promoter on aluminum substrate. It was reported that the thicknesses of the silane film at curing temperature of below 50°C, or above 93°C, are quite different. At higher curing temperature, the film is thinner [5]. Adams et al [49] compared the effect of curing temperature of the silane film on adhesion joints, and their results did not show a significant difference between 40°C curing and 93°C for the Gc values for both "dry" and "wet" conditions.

  Interestingly, temperature treatment may have a "flip-flop" effect

shown by George et al. [50]. XPS study showed that interface formed between silicon and APS, the orientation of the organosilane was changed upon heat treatment from interacting with the amino side to forming covalent bonding with the silanol side.

- Concentration of the solution

  Kaul et al. examined the influence on the durability of $Al_2O_3$/polyethylene joints primed by APS [51]. It was found that for APS, higher concentration would promote defect formation within the silane interphase, while low solution concentrations promote a more uniform layer. When the concentration is too low, <0.5%, the coverage of the substrate surface may be incomplete.

- Type of solvent and time for hydrolysis

  Controling the aging time of the organosilane solution is of paramount importance to obtain the optimum properties of adhesive joints. Several studies have been conducted to evaluate the hydrolysis time for silane solutions [52, 53]. For methoxy groups hydrolysis happens quickly. Therefore, condensation or polymerization could happen if the aging time is too long. It has been reported that for 1% GPS aqueous solution, after 9 hours of hydrolysis, the concentration of oligomers is over 60% [4]. Bertelsen et al. [55] also suggested to use 1% GPS solutions should be

within 10 hours. After 8 hours the solution can not be used to obtain same adhesion promoter effects. Fresh solutions should be used at all the time.

- Rinsing protocol

APS was used to study the effect of rinsing on the nature of the silane layer deposited by Abel et al. [3]. It was found that very different adsorption behavior depending on the rinsing protocol employed (including water, methanol or no rinsing). Rinsing with water would form a thicker layer of organosilane on the aluminum surface than rinsing with methanol. It is possible that the organosilane species have a better dissolution in methanol, or instantaneous reaction of APS with water happen at the surface. A critical quantity of water is required in the solution to allow hydrolysis take place.

The thickness of the deposited organosilane films ranges from 2nm to 5nm for these three rinsing protocols. For APS on aluminum substrates, the thickness of the film decreases in the order of no rinsing, rinsing by water or methanol They also used Beer-Lambert relationship to calculate the film thickness and get that by changing from water rinsing to methanol rinsing, the film thickness would decrease 50% [3].

- pH value of the solution

The pH of organosilane solution can influence the nature of the various reactions that occur in solution [1,58]. PH values from 3 to 11 were investigated by the use of acetic acid/sodium hydroxide alkali adjustments as appropriate by Abel et al. [48]. Fig. 2.9 and Table 2.2 show that the wedge test crack growth for various solution pH values for GPS solutions. Another test is: for silane concentrations from 0.1% -12%, fracture energy, $G_{Ic}$, data obtained from the longest exposure time. These two tests combined together and showed pH 5.0 gives the best performance of the GPS solution [48].

#### *2.4.3.3 Use of dipodal organosilanes*

Plueddemann proposed the use of bis-silanes (dipodal) to crosslink films of a monosilane [1]. An alternate approach is to use 2 layers of silanes on the substrate surface. This requires coating the substrate with dipodal organosilane first, then after air drying, apply the monosilane on top of it. This two-step treatment was used by Tilset and Song et al. [56, 56], who used 1,2-bis[triethoxysilyl] ethane (BTSE) as the dipodal orgnaosilane. It was found that using BTSE can greatly improve corrosion resistance of the aluminum substrates. The corrosion protection of aluminum substrate is better than chromate conversion coating.

Song et al. [57] concluded that the two-step treatment (BTSE and APS)

and BTSE only, form a dense hydrophobic interfacial layer at the top of the substrate, which plays a major role in the corrosion protection of aluminum. Fig. 2.10 and Table 2.3 compare the corrosion resistance results of various treatments and reveals that the two-step treatment of aluminum surface provided excellent corrosion resistance [56].

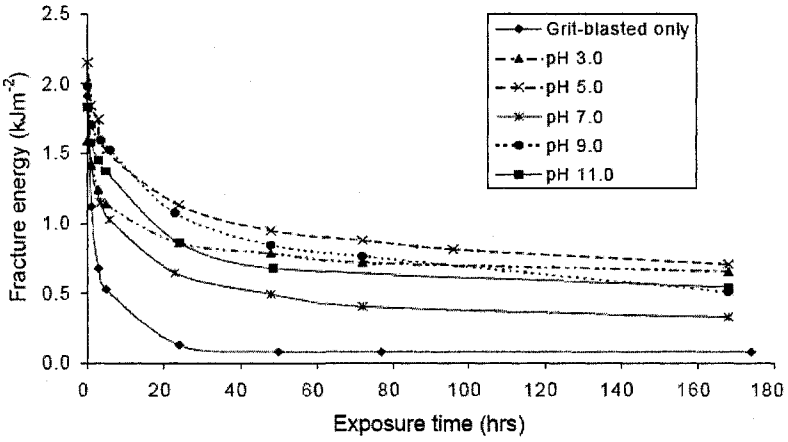


***Figure 2.9*** *Boeing wedge test crack growth for various solution pH value [48].*

**Table 2.2** the effect of pH on 168 hours fracture energy for 0.1, 1 and 12% silane concentrations [48].

| Sample pH | 168 h fracture energy ($kJm^{-2}$) | | |
|---|---|---|---|
| | 0.1% silane | 1% silane | 12% silane |
| 3 | 0.142 | 0.655 | 0.183 |
| 5 | 0.427 | 0.708 | 0.130 |
| 7 | 0.208 | 0.290 | 0.569 |
| 9 | 0.210 | 0.509 | 0.468 |
| 11 | 0.164 | 0.541 | 0.387 |

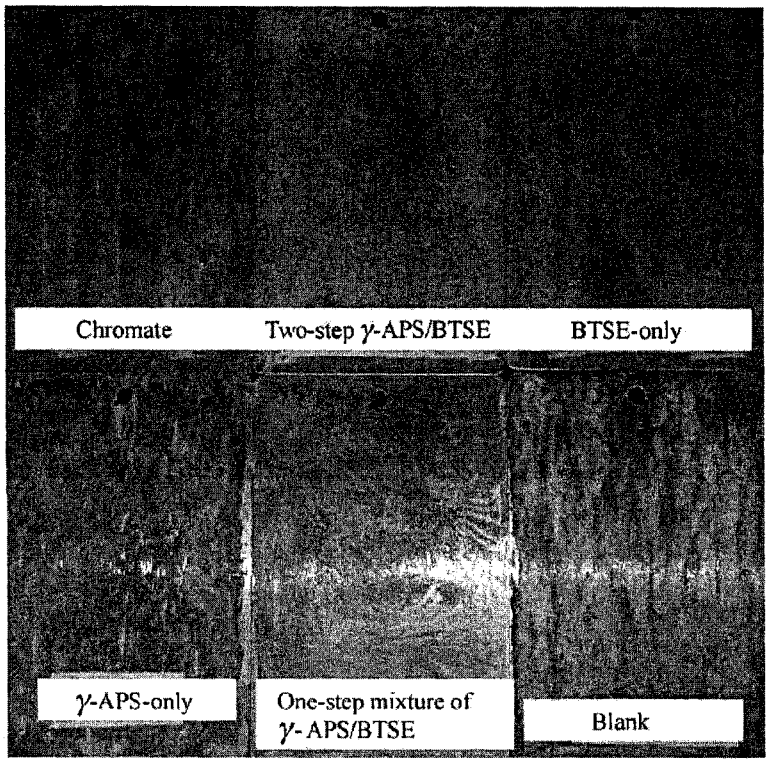


Panels of aluminum 3003 after 336 days in salt spray test.

***Figure 2.10*** *Panels of aluminum 3003 after 336 hours in salt spray test [56].*

**Table 2.3** Salt spray test results for aluminum alloy 3003 after exposure for 336 hours [56]

| ID | Treatment | Corroded area (%) |
|---|---|---|
| 0 | Blank | 100 ± 0 |
| 1 | γ-APS 2%, pH 10.6 | 90 ± 0 |
| 2 | γ-APS 5%, pH 10.6 | 90 ± 5 |
| 5 | Mixture γ-APS 1.6% + BTSE 0.4%, pH 6 | 80 ± 0 |
| 6 | Mixture γ-APS 5% + BTSE 1.25%, pH 6 | 75 ± 5 |
| 9 | Two step: 1st BTSE 1.6%, pH 6; 2nd γ-APS 0.4%, pH 6 | 20 ± 5 |
| 10 | Two-step: 1st BTSE 5%, pH 6; 2nd γ-APS 5%, pH 6 | 15 ± 5 |
| 13 | BTSE 1.6%, pH 6 | 20 ± 5 |
| 14 | BTSE 5%, pH 6 | 15 ± 5 |
| 15 | Chromate | 10 ± 10 |

### *2.4.3.4 Interfacial diffusion of moisture*

Zanni-Deffarges and Shanahan [59] have suggested that water diffuses faster at the interface between substrate and polymer. They found that a significantly higher diffusion coefficient (almost an order of magnitude) for moisture diffusing along adhesive joints than in bulk specimens. They postulated the diffusion within the adhesive joint was occurring by another route, as well as by conventional diffusion within the polymer. It was suggested that water can enter the system by seepage close to the interface or in the interfacial region by a phenomenon called 'capillary diffusion'. Since the glass represents a relatively high energy surface, the interfacial free energy of substrate-dry adhesive could well be quite large and, as a consequence, a significant interfacial tension could help to pull the water diffusion front into the system so it was found that the moisture diffuses into the interface much faster than the bulk.

A study by Wu et al. [60] found that excess water was discovered within 30Å of the metal/polymer interface. The water concentration at the interface reached 17% (by volume) for the samples without a coupling agent and 12% for the ones with coupling agent. Beyond the interface, the water

concentration was at 2 to 3%, which is typical of bulk polyimide.

In the study by Yim et al. [60], neutron reflectivity experiments show that the distribution of water within the silane layer is not uniform. A thin, water rich layer is present adjacent to the silicon oxide surface, while a much lower level of water is present in the remainder of the silane finish and in epoxy overcoat layer.

## 2.5 Previous work in our group

### 2.5.1 Bulk treatment vs. surface treatment

D. Narsavage-Heald compared the effect of organosilane treatments in the bulk epoxy resin versus on the substrate surface. The silane treatment at the surface resulted in much better adhesion for both "dry" and "wet" conditions. Among the silane coupling agents evaluated, APS and GPS provided the best improvements in adhesion [61].

### 2.5.2 Comparison of adhesion promoters

Khayankarn [6] studied several epoxy systems and bonded to borosilicate glass coated with various silane coupling agents. Flow microcalorimetry was used to directly observe the strength of probe molecules onto surfaces, and thus characterized surface reactivity. It was found that both

the heat of adsorption (bond strength) and active site density play important roles in prediction of adhesive strength (dry). Attenuated Total Reflection Infrared Spectroscopy and X-ray Photoelectron Spectroscopy techniques were also used to characterize the locus of failure. These results indicate that the debonding path is in the epoxy/silane interphase region. Before aging, the crack propagates closer to epoxy layer. After aging, the crack propagates closer to the glass surface. In her study, it was also found that the apparent diffusion coefficient of epoxy adhesive in the DCB specimen is significant higher than that of epoxy film.

## 2.6 References


1. A. V. Pocius, Adhesion and Adhesives Technology, an introduction, Hanser Publishers, Munich Vienna New York, (1997).

2. E. P. Plueddemann, Silane Coupling Agents. New York: Plenum Press. (1982).

3. M. L. Abel, J. F. Watts, R. P. Digby, Intl. J. Adhesion & Adhesives 18 179-192, (1998).

4. M. L. Abel, J. F. Watts, R. P. Digby, The Journal of Adhesion, 80:291-

312, (2004).

5. M. L. Abel, A. Rattana, and J. F. Watts, J. Adhesion 73, 313-340 (2000).

6. O. Khayankarn, Ph.D. Dissertation, Lehigh University, Bethlehem, PA, USA, 2004

7. A. J. Kinloch, Adhesion and Adhesives: Science and Technology. London: Chapman and Hall. (1987).

8. F. L. Matthews and R. D. Rawlings, Composite Materials: Engineering and Science. Cambridge, England: Woodhead Publishing, (1999).

9. A.A. Griffith. A. A. Griffith, Philosophical Transactions of the Royal Society of London, Series A, Mathematical and Physical Sciences, 221: p. 163, (1920)

10. H. Dannenbrg, J. Appl. Polymer Sci., 5, 125, (1961).

11. A. N. Gent, and A. J. Kinloch, Journal of Polymer Science, Part A: Polymer Chemistry, 9: p. 659, (1971).

12. W. J. van Ooij and A. Sabata, Surf. Interface Anal. 20, 475 (1993).

13. K. L. Mittal, (Ed.), Silane and Other coupling Agents, Vol. 2. VSP, Utrecht (2000)

14. M. R. Rosen, Journal of Coating Technology, 50: p. 644, (1978).

15. P. W. Erickson, and E. P. Plueddemann, Composite Materials. Vol. 6. New York: Academic Press, (1974).

16. W. Southeng, Polymer Interface and Adhesion. New York: Marcel Dekker, (1982).

17. P. Walker, J. Adhesion Sci. Technol. 5, 279 (1991).

18. E. P. Plueddemann, J. Adhesion Sci. Technol. 5, 261 (1991).

19. R. Chen and F. J. Boerio, J. Adhesion Sci. Technol. 4, 453 (1990).

20. J. C. Bolger, and A. S. Michaels. Interface Conversion for Polymer Coatings, ed. a.G.D.C. P. Weiss. New York: American Elsevier, (1969).

21. E. P. Plueddemann and G. L. Stark. Mod. Plast. 51 (3), 74 (1974).

22. Technical Bulletin KR-1084-2, Kenrich Petrochemicals, Inc., Bayonne, (1987).

23. C. A. Kumins and J. Roteman, J. Polymer. Sci., Part A 1, 527 (1963).

24. J. Gaehde. Plaste Kautschuk 22 (8), 626 (1975).

25. E. P. Plueddemann. SPI, 29th Ann. Tech. Conf. Reinf. Plast. 24-A (1974).

26. E. P. Plueddemann, Journal of Paint Technology, 42: p. 600, (1970).

27. P. Walker, Journal of the Oil and Colour Chemists' Association, 65: p. 436, (1982).

28. P. Walker, Journal of the Oil and Colour Chemists' Association, 66: p. 188, (1983).

29. P. Walker, Journal of the Oil and Colour Chemists' Association, 67: p. 108, (1984).

30. P. Walker, Journal of the Oil and Colour Chemists' Association, 67: p. 126, (1984).

31. P. Walker, Journal of the Oil and Colour Chemists' Association, 5: p. 279, (1991).

32. J. D. Miller and H. Ishida, Silanes, Surfaces and Interfaces, vol. 1 of the proceedings of the silanes, surfaces and interfaces symoposium, D. E. Leyden, Ed. Snowmass, Colorado, 19-21, Gordon and Breach Science Publishers, London, (1985).

33. H. Schmidbaur, Angew, Chem. 4, 201-211 (1965).

34. H. Schmidbaur and M. Schmidt, J Am. Chem. Soc. 83 2963-2964 (1961).

35. F. J. Boerio, C. A. Gosselin, R. G. Dillingham, and H. W. Liu, J. Adhesion 13, 159-176 (1981).

36. F. J. Boerio, and C. A. Gosselin, advances in Chemistry Series 203, 541-558 (1983).

37. R. Brindle, M. Pursch, and K. Albert, Sol. State NMR 6, 251-266 (1996).

38. F. Bauer, A. Freyer, H. Ernst, H. J. Glasel, and R. F. Pratt, J. Am Chem. Soc. 102, 1859-1865 (1980).

39. Y. L. Leung, M. Y. Zhou, P. C. Wong, K. A. R. Mitchell and T. Foster, Appl. Surf. Sci. 59, 23-29 (1992).

40. Y. L. Leung, Y. P. Wang, P. C. Wong, K. A. R. Mitchell and T. Foster, J. Mat. Sci. Lett. 12, 844-846 (1993).

41. B. Willians, British Steel internal reports, and Stematic study of the effect of deposition conditions for organosilane coverage on Zinc Coated Steel, British Steels Strip Products, West Glamorgan, UK, September (1995).

42. M. Gettings and A. J. Kinloch, Surf. Int. Anal. 1, 189-195 (1979).

43. W. Thiedman, F. C. Tolan, P. J. Pearce, C. E. M. Morris, J Adhes

22:197, (1987).

44. A. A. Baker, R. J. Chester, Int J Adhes Adhes 12:73, (1992).

45. R. J. Kuhbander, J. J. Mazza, SAMPE Symp 38:1225, (1993).

46. D. R. Arnott, M. R. Kindermann, J Adhes 48:101, (1995).

47. R. P. Digby and S. J. Shaw, Int. J. Adhes. Adhes. 18, 261-264, (1998).

48. M. L. Abel, R. D. Allington, R. P. Digby, N. Porritt, S. J. Shaw and J. F. Watts, International Journal of Adhesion and Adhesives; 26, 2-15, (2006).

49. A. N. N. Adams, A. J. Kinloch, R. P. Digby and S. J. Shaw, Proceedings of the adhesion society annual meeting. Vol 23, 219, (2000).

50. I. George, P. Viel, J. Suski and G. Lecayon, Surf. Interface anal. 24, 774-780 (1996).

51. A. Kaul, N. H. Sung, I. Chin, C. S. P. Sung, Polym. Eng Sci, 24;493, (1984).

52. H. Ishida, Polym Compos, 5:101, (1984).

53. C. M. Bertelsen, F. J. Boerio, J Adhes 70:259, (1990),

54. M. S. Kent, E. D. Reedy, H. Yim, A. Matheson, J. Sorenson, J. Hall, K.

Schubert, D. Tallant, M. Garcia, T. Ohlhausen, R. Assink, Using self-assembling monolayers to study crack initiation in epoxy/silicon joints. Journal of Materials Research 19(6), 1682-1695 (2004)

55. C. M. Bertelsen and F. J. Boerio, Prog. Org. Coat. 41,239-246 (2001)

56. B. G. Tilset, A. Bjorgum, F. Lapique, C. J. Simensen, Proceedings of the Annual meeting of the Adhesion Society, 25th, 177-179, (2002).

57. J. Song, W. J. van Ooij, J. Adhesion Sci. Technol. Vol. 17, No.16 pp.2191 (2003).

58. G. Tesoro, Y. J. Wu. Adhes Sci Technol 5: 771, (1991).

59. M. P. Zanni-Deffarges, and M. E. R. Shanahan, International Journal Adhesion and Adhesives, 15, 137, (1995)

60. Wu, Wen-Li; Orts, William J.; Majkrzak, Charles J.; Water Hunston, Donald L., Polymer Eng. and Sci., vol 35, (12); 1000-1004, (1995).

61. D. Narsavage-Heald, and R. A. Pearson. *Proceeding 24th Annual Meeting of The Adhesion Soc.* 2001.

# CHAPTER 3

# EXPERIMENTAL APPROACH

---

This research is focused on the moisture ingress in epoxy adhesive joints and the subsequent adhesion loss. Samples were prepared by sandwiching epoxy resin between glass slides and then cured by heat or UV radiation. The cured samples were then put in an environmental chamber with controlled temperature and humidity for hygrothermal aging. The adhesive strength of the joints was measured at various aging time periods. XPS and SEM Analysis of the fracture surfaces of the adhesive joints were used to characterize how moisture progressee into the epoxy/glass adhesive joint.

## 3.1 Materials

The developmental sealant G3PS1 by National Starch Chemicals & Co. was used in this research project to study the adhesion loss of DCB specimens. It is a UV-curable sealant with excellent barrier properties and low weight gain under humid conditions. However, because most commercial adhesives and coatings are complex blends of epoxy resins, curing agents, and additives that

make the study of the underlying physics difficult. For this work, epoxy model systems were also chosen with simple chemistries that are often found in commercial resins. The resin system consists of Bisphenol F epoxy (BisF) resin cured with 2,4-ethylmethyl Imidazole (2,4-EMI). The epoxy resins were premixed and stored in syringes at -40°C. The adhesion promoters used were glycidoxypropyltrimethoxysilane (GPS), (3-Aminopropyl) triethoxysilane (APS), Bis(trimethoxysilylpropyl) Amine (BTSPA), Bis(triethoxysilane) Ethane (BTSE) purchased from Gelest and used as received. Borosilicate glass (BOROFLOAT) from Erie Scientific Company was used in this study as the substrate for epoxy. The glass was received in the form of 12.7x76.2x0.32 mm slabs.

## 3.2 DCB sample preparation

### 3.2.1 Glass sample surface treatment

Organosilanes adhesion promoters were diluted to a final concentration of 1% by weight in 95% methanol/5% water. After preparation, the solution is agitated using magnetic stir to facilitate hydrolysis. The pH of the solution was adjusted to 4 by adding acetic acid. The hydrolysis time for GPS and APS was between 2 to 4 hours, and for BTSE and BTSPA was 24 hours. Glass plates are cleaned by isopropyl alcohol to degrease. The bottom glass plates of the DCB samples are sputter coated by Au/Pd for a 12x17mm area at one end to create a weak interface for the future initiation of a sharp crack. Then the glass plates are cleaned by UV/$O_3$ for 20 minutes to remove organic contamination.

**Table 3. 1** Chemical structures of materials used in the experiments.

| Chemical Name | Chemical Structure |
|---|---|
| Diglycidyl ether of bisphenol F | 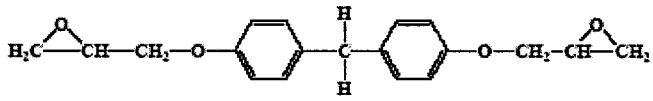 |
| 2, 4 EMI | 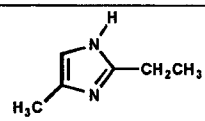 |
| Glycidoxypropyl-trimethoxy silane (GPS) | 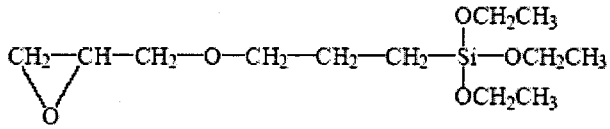 |
| (3-Aminopropyl) triethoxysilane (APS) | 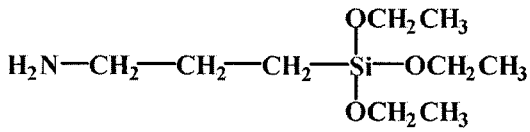 |
| Bis(triethoxysilane) Ethane | 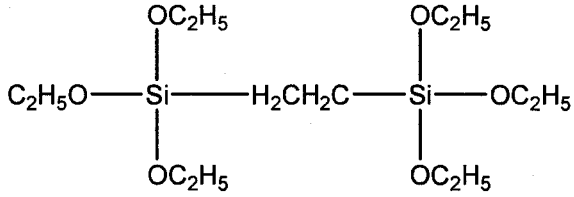 |
| Bis(trimethoxysilyl-propyl) Amine, | 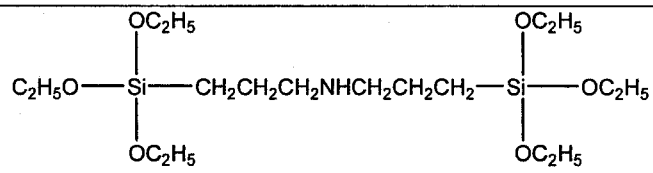 |

Glass plates are dipped into silane solutions for 2 minutes, rinsed by methanol to remove excess silane coupling agent, air dried for 10 minutes, then baked at 110°C for 8 minutes.

### 3.2.1 Preparation of DCB specimens

A spacer by 2x10mm is placed on each end of the bottom glass plate. Adhesive is applied on the bottom glass plate. The top glass plate is placed on the top and a medium binder clip is used on each end to set the specimen in place. The prepared specimens are cured by following the appropriate cure procedure.

### 3.2.3 Curing of epoxy systems

As mentioned previously, two epoxy systems were investigated in this project. The first epoxy system is BisF/EMI epoxy that is a thermally cured system, and represents a model sealant. The curing condition is 60°C for 4 hours, and then 150°C for another 2 hours. The other epoxy system is NSC G3PS1, which is generously supplied from National Starch, Company, Bridgewater, NJ. This is a developmental UV cured epoxy sealant system. It is cured under UV radiation at 35mW/cm$^2$ for 4 minutes on each side of the DCB specimens. The UV lamp used here is Loctite® ZETA® 7411 UV flood system (Figure 3. 1). The unit contains a 4 inch, 400 Watt Metal Halide Bulb. The curing was performed under the UV light source at a distance of 12 cm.

The UV radiation intensity was approximately 35mW/cm$^2$. The spectral output of UV metal halide bulk is shown in Figure 3.2 [1].

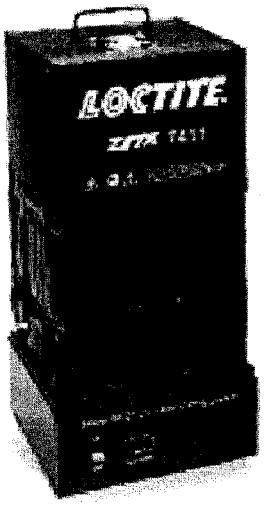


***Figure 3. 1** The Loctite® ZETA® 7411 UV flood system [1].*

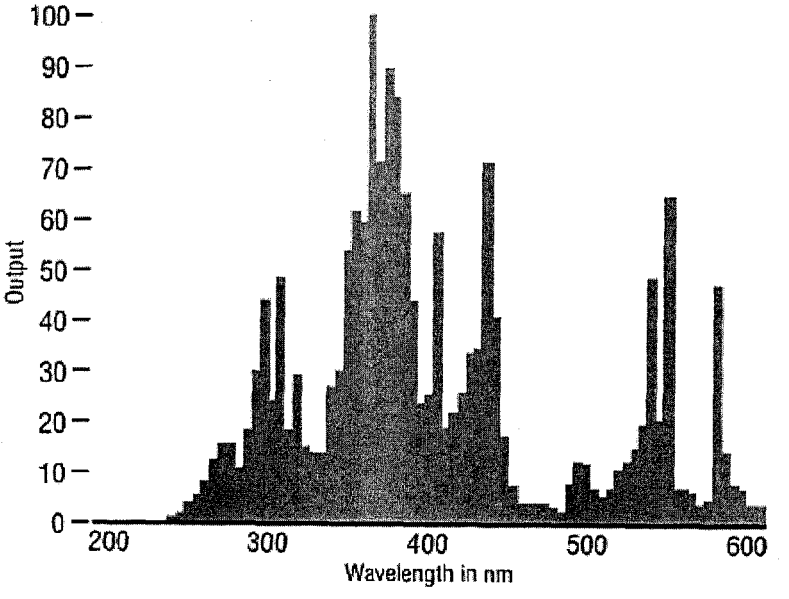


***Figure 3. 2** The spectral output of UV metal halide bulk.*

### 3.2.4 Polishing of DCB samples

Normally, the adherend material, the beam, in a DCB test is metal, ceramic, and other strong and tough materials. Glass is brittle comparing with these materials. Because the strength of epoxy/glass adhesion force is strong enough to compare with the strength of glass, the glass pieces of DCB samples are often fractured during the test and result in failure of measurement. One of the main causes of the breaking of glass piece is because of the defects on the edge of the glass piece, which generate stress concentrations. Our solution to this problem is to polish the sides of glass pieces and make it defect free down to micrometer level. After curing, the specimens are grinded then polished down to 1 micron on both sides of the specimens. It is experience that the polishing step is crucial important to consistently generate reliable data from epoxy/glass adhesive joint DCB tests.

### 3.2.5 Hygrothermal aging

DCB specimens are exposed to moisture in a Dispatch Ecosphere Series controlled humidity chamber at 85°C and 85% relative humidity (RH) for different periods of time in order to study effect of hygrothermal aging time on adhesive strength.

## 3.3 Measurement of adhesion strength

DCB testing was performed using a computer control screw driven Instron testing machine (model 5521) in displacement control, at a speed of 0.127 mm/min, with 500 N load cell. Tensile force was applied at the end of a specimen in a direction normal to the crack surface which is called cleavage As the load was applied, the crack propagated, leading to a load drop, then unloaded further using the crosshead position and subsequently reloaded using crosshead position. This cycle was repeated in order to get several strain energy release rate ($G_C$) values for averaging.

## 3.4 Surface characterization

After the test, the DCB sample is opened and epoxy bonding layer and glass surface that was bonded to adhesive are exposed and available for further analysis. By analyzing the atomic component of these surfaces, one can find out the exact location that the debonding started and propagated. For example, for adhesive failure, visually, the debonding is happened at the glass surface, but actually may happen on the adhesive side or adhesion promoter layer. Surface analysis of the glass surface from debonded sample can give an answer and a lot more detailed and accurate information. That requires an analysis

method that only sensitive to the very surface of the sample. The following are some instruments that very powerful in analyze material surfaces and some of them were used in this research.

### 3.4.1 X-ray photoelectron spectrum (XPS)

In this study, XPS was applied to characterize both the epoxy side and the glass side of the fracture surfaces in order to reveal the locus of failure. The fracture surfaces of BTSE/GPS two-step treated DCB specimens at 0 and 9 days after hygrothermal aging were examined using XPS, which is considered the most surface sensitive technique, in order to obtain the more precise compositions at the fracture surfaces. All XPS data were obtained with monochromatic Mg Kα radiation and photoelectron takeoff angle of 90°. At this takeoff angle, the sampling depth is about 3.6 nm [2].

X-ray photoelectron spectroscopy (XPS) is widely used in the characterization of the chemistry of the surface of solid materials. XPS is based on photoelectric effect: an electron may escape from a material surface after absorbing a high energy photon, X-ray in this case, and the escaped electron carries information of the information of origin atom it escapes from. XPS spectrum shows the kinetic energy and number of electrons that escape from the material surface after absorbing a high energy photon of X-ray. Normally, only electrons from a very thin layer (1-10nm) of the material surface can

escape. Deeper photo-emitted electrons are either recaptured or trapped in various excited states within the material. Thus, the result of XPS spectrum only shows the chemical structure of the very top surface of a material [4].

Following schematic drawing shows the key components of a XPS and how it works. Most commercial XPS used either a highly focused 20 to 200 micrometer beam of monochromatic aluminum K-alpha X-rays or a broad 10-30 mm beam of non-monochromatic (achromatic or polychromatic) magnesium X-rays. As an X-ray beam shine on a sample surface, the energy of X-ray photon may be adsorbed by a core electron of an atom. When the energy that the electron obtained from the X-ray photon is higher than the binding energy of the electron to its nuclear, the electron will escape from the atom with the expense of a part of the adsorbed energy (work function $\phi$), and the remaining energy is carried away with the electron as its kinetic energy ($E_k$). A high vacuum is needed to accurately measure the escaping electron kinetic energy. With this information, the binding energy ($E_b$) of the electron to material surface can be calculated by the Einstein relationship:

$$E_b = h\nu - E_k - \phi \tag{3.1}$$

The work function $\phi$ can be compensated artificially, and $E_k$ and

corresponding number of electrons is measured and recorded by detector, which gives the XPS spectrum.

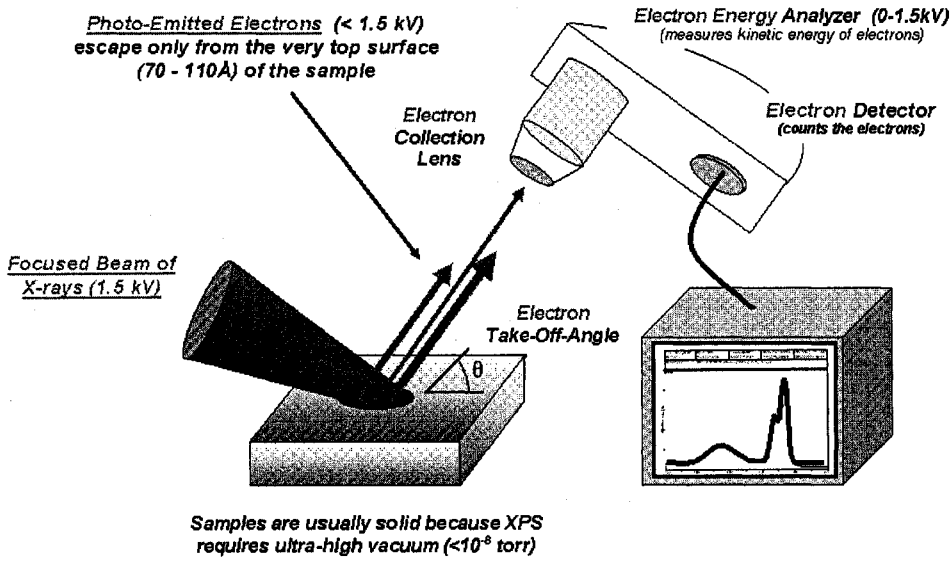


***Figure 3. 3** Components and Working Concepts of XPS*

The binding energy of the core electron is unique for each element. Thus the XPS spectrum is used to identify element type (from binding energy) and the empirical formula (ratio between the numbers of electrons at different specific $E_b$). The probabilities of core electrons to adsorb X-ray photon in different element atoms are different. There is a discrimination of escaping electron population from different element atoms. Thus, to generate atomic

percentage values, each raw XPS signal must be corrected by dividing its signal intensity (number of electrons detected) by a "relative sensitivity factor and normalized over all of the elements detected.

Binding energy is also varied by the chemical environment of the atom (chemical shift). Therefore, the information of the chemical or electronic state of each element on the surface is also disclosed with XPS spectrum.

XPS is a relatively highly sensitive and accurate method for surface characterization. Under optimum conditions, and calculated from the Major XPS Peaks, the quantitative accuracy of the atom % values is 90-95%. The accuracy can be further improved if a high level quality control protocol is used. At routine conditions, the accuracy of 80-90% of the value reported in atom % values may be expected. If calculation is based on weaker peaks that just have 10-20% of the strongest peak, the accuracy ranges about 60-80% of the true value. And usually the detection limit of XPS is 0.1-1.0 atom%

Besides giving a general element composition of a material surface, XPS can measure a line profiling or mapping of an area of the surface and give the uniformity of elemental composition across the top the surface. Although XPS can only show information of the very top surface (<10 nm) of a material, with the aid of ion beam etching, a depth profiling of element and electron or

chemical state can be obtained up to 1000 nm. It takes 1–4 hours for a depth profile that measures 4–5 elements as a function of etched depth, while normal XPS test takes 1–10 minutes for a survey scan that measures the amount of all elements, and 1–10 minutes for high energy resolution scans that reveal chemical state differences. Depth profile may also be obtained tilting the sample, that is also called angle resolved XPS.

Figure 3.4 shows the survey scan of adhesion promoter coated microscope glass slide. Figure 3.5 is the high energy resolution scan of the same slide. The relative ratio of different atoms in the surface of the microscope slides can be calculated by the software, and thus information about exact chemicals on the surface can be obtained. XPS is extensively used in current research to characterize the surface chemistry of adhesion promoter treated glass surface as well as the fracture surface of an adhesive joint after DCB test to find out where exactly the bonding failed during tests, and possible chemistry change during hygrothermal aging.

Scienta ESCA 300 is generally regarded as one of the best XPS instruments in operation today.

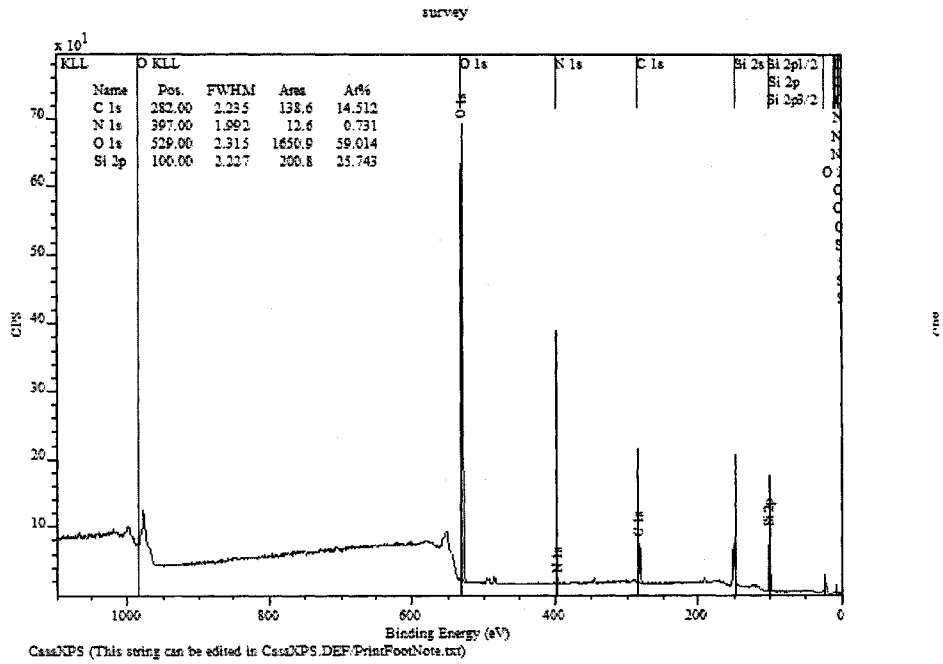


***Figure 3.4*** *XPS survey scan of an adhesion promoter coated microscope glass slide.*

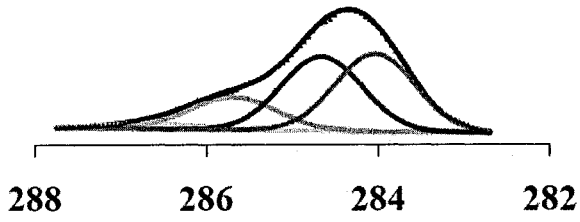


***Figure 3. 5*** *XPS the high energy resolution scan of an adhesion promoter coated microscope glass slide*

### 3.4.2 Scanning Electron Microscope (SEM) JOEL 6300F

JOEL 6300F is a high resolution field emission scanning electron microscope. This SEM instrument has high brightness source, which allows considerable flexibility in the types of imaging techniques. The extremely fine electron source of the field emission system ensures high resolution images from this instrument. Useful magnifications in excess of 200,000 times are obtainable, which translate to a resolution of 1.5 nm at accelerating voltage.

The high brightness of this source also allows high resolution imaging and characterization of beam sensitive materials at high magnifications at very low accelerating voltages.

Figure 3. **6** is a picture of the SEM used to study the fracture surfaces of the DCB specimens.

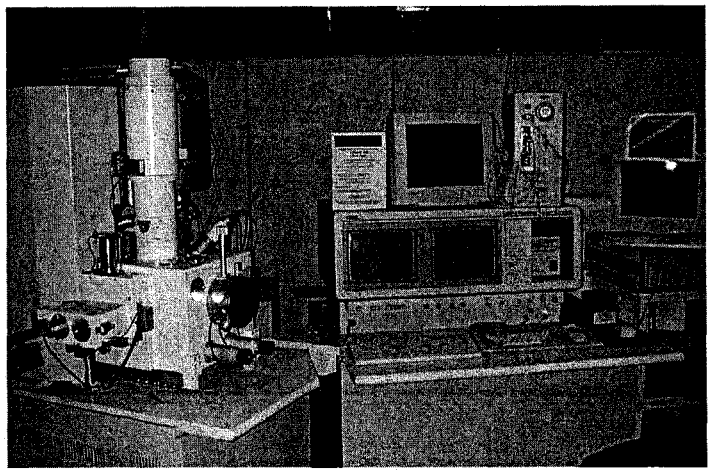

***Figure 3. 6** SEM JOEL 6300F used in this project.*

## 3.5 References


1. Manuel of Loctite ZETA 7411 UV flood system
2. D. Briggs, Application of XPS in Polymer Technology. 2nd ed. Practical Surface Analysis, ed. D briggs, and M.P. Seah. New York: John Wiley & Son. (1990).
3. http://www.eaglabs.com/enUS/presentations/TOFSIMS/Presentation_Files/index.html
4. L. T. Lee, E. K. Mann, D. Langevin,, Farnoux, B., Langmuir, 3076-3080, (1991)
5. T. P. Russell, Mater. Sci. Rep. 5, 17, (1990).
6. H. Yim, M. S. Kent, J. S. Hall, J. J. Benkoski and E. J. Kramer, J. Phys. Chem. B 106, 2474-2481, (2002).
7. Kent, M. S.; Yim, H. Silanes and Other Coupling Agents; Mittal, K. L., Ed.; VSP: Utrecht, The Netherlands, Vol. 2, (2000)
8. Kent, M. S.; Smith, G. S.; Baker, S. M.; Nyitray, A.; Browning, J.; Moore, G.; Hua, D.-W. J. Mater. Sci. 31, 927, (1996).
9. R. A. Pearson, T. B. Lloyd, H. R. Azimi, J. Hsiung, M. S. Early, and P. D. Brandenburger, IEEE Transactions on Components, Packaging, and Manufacturing Technology, Part A, 20: p. 31, (1997).
10. T. B. Lloyd, Colloids and Surfaces A: Physicochemical and

Engineering Aspects, 93: p. 25, (1993).

11. A. N. Gent, and A. J. Kinloch, Journal of Polymer Science, Part A: Polymer Chemistry, 9: p. 659, (1971).
12. A. A. Griffith, Philosophical Transactions of the Royal Society of London, Series A, Mathematical and Physical Sciences, 221: p. 163, (1920)
13. A. J. Kinloch, Adhesion and Adhesives: Science and Technology. London: Chapman and Hall, (1987).

# CHAPTER 4

# USING DIPODAL ORGANOSILANES TO IMPROVE MOISTURE RESISTANCE OF EPOXY/GLASS INTERFACES

---

The adhesion of thermally cured epoxy (Bisphenol F/2,4 EMI) system with borosilicate glass was studied. Several treatments of glass surfaces were investigated for the purpose of improving the moisture resistance of the epoxy-interface. Parameters affecting loss of adhesion at the interfaces were evaluated. XPS was used at the fracture surfaces to determine the locus of failure for a two-step silane surface treatment.

## 4.1 Background

### 4.1.1 One layer of organosilane

When epoxy bonded joints are exposed to an aqueous environment, the interphase of the joint is susceptible to moisture attack [1]. To solve this problem, organosilanes can be used to improve adhesion between epoxies and

inorganic substrates [2, 3, 4]. The organosilane normally contain one alkoxy chain and 1-3 Si-OR groups. Once hydrolised, organosilanes Si-OH groups can react with inorganic substrates and the other functional groups on the organosilane molecules can react with organic materials. Covalent bonds are formed and help form a stronger bond. Watts and Kinloch used ToF-SIMS to provide direct evidence of the covalent bonds at the interface [5]. Application of organosilanes as a more environmental friendly method on metal surface is a good replacement of previous toxic treatments [4, 6, 7, 8, 9, 10]. Organosilane coupling agents have been used for many years to increase the adhesion between epoxy matrix and glass fibers and for corrosion protections [2]. Many studies have been conducted on aluminum for corrosion protection in aerospace related applications. [3].

During the application of organosilane, a subtle change in the procedure can lead to very different results of the adhesion promotion. This is a major cause for different reports of adhesion properties seen from various workers in this field [11,12,13]. The processing parameters of the application of organosilane adhesion promoters were evaluated to obtain optimum results of adhesion of the joints and moisture resistance of bonded joints or metal surfaces exposed to water, including solution pH [14], silane concentration [11,15,16], water concentration in the solvents [16], hydrolysis time [17, 18],

drying time and temperature [15,19,20], time lag between silane application and bonding, rinsing protocols after silane application [11], etc. Optimizing application parameters is vital to the final testing results. The "International Collaborative Program on Organosilane Adhesion Promoters" (ICOSAP), which has involved sixteen research groups in six countries, investigated the relationships between silane application variables, solution chemistry, surface chemistry, joint durability and mechanisms of failure [10,11,12,13,21,24].

APS and GPS are the most thoroughly studied adhesion promoters. They are often used for improving adhesion of polymeric matrix and fibers, or on aluminum for aerospace repair purposes [4]. Within ICOSAP, scientists investigated aqueous solution of γ-glycidoxypropyl trimethoxysilane (γ-GPS) to examine the effects of silane solution concentration, pH, hydrolysis time, drying time and temperature, substrate hydration, and processing time lags between application and bonding, on bond strength and durability. The effect that each variable has on the process and the resulting integrity of the GPS/aluminum interface were reviewed. The formation of covalent interfacial bonding is a function of the hydrolysis and condensation of the silane molecules in solution as well as the type of solvent used. The curing temperature of the aqueous film on the aluminum also has an effect on the chemistry of the resulting primer film and its efficacy as an adhesion promoter [5]. C. M. Bertelsen and F. J. Boerio investigated the effect of processing

variables of GPS. They used FT-NMR to study the hydrolysis and condensation process on the molecular structure of GPS aqueous solution. They found that hydrolysis is a very rapid process, and the rate could be controlled by adjusting pH of the solution [24]. Their research offered valuable information for determining application conditions of organosilane. The details of the effects of application parameter were summarized in Chapter 2. Table 1 includes optimum processing conditions of GPS.

### 4.1.2 Two step surface treatment used for corrosion resistance

The use of organosilane greatly improves the adhesion between epoxy and inorganic materials [4]. Most of those applications involved the use of one type of organosilane applied on inorganic substrate [12]. Song et al. [3] and Tilset et al. [56, 26] found that applying 2 layers of organosilanes, including one organosilane with 3 silanols and one dipodal silane with 6 silanols, can greatly improve corrosion resistance in salt spray tests and filiform tests. Films of γ-aminopropyltriethoxysilane (γ-APS), 1,2-bis[triethoxysilyl] ethane (BTSE) and their mixtures adsorbed onto pure aluminum from aqueous solutions were characterized by means of ellipsometry, infrared spectroscopy(IR) and X-ray photoelectron spectroscopy (XPS). It was found that after hydrolysis in water the silanes were readily adsorbed onto aluminum oxide surfaces initially forming hydrogen bonds. Upon curing, such bonds are replaced by metallosiloxane bonds, Si-O-Al. The remaining silanol groups in

the film condense and form Si-O-Si bonds. As the Si-O-Al bonds are known to hydrolyze, the corrosion protection is related to the hydrophobicity of the siloxane films formed on the metal substrate. BTSE films are acidic as they contain free silanol groups, therefore they are compatible with some organic paints so they could provid better corrosion protection on aluminum substrates as compared with the common but more toxic chromate treatment [3].

### 4.1.3 Objectives

The goal of this project is to study the various factors that affect adhesion loss under hygrothermal aging conditions and to provide insight into the mechanisms affecting adhesion loss.

Specifically, the objectives of this project include:

- Using a mixture of dipodal and monosilanes to treat glass surface and evaluate adhesion at both dry and wet conditions
- Using a two-step organosilane treatment to treat glass surface and evaluate adhesion at both dry and wet conditions
- Compare the adhesion loss of filled versus unfilled epoxy systems
- Compare the loss of adhesion of adhesive joints at various bondline thickness

## 4.2 Materials

For this work, epoxy model systems were chosen with simple chemistries that often found commercial resins. The system consists of Bisphenol F epoxy resin cured with 2,4 EMI. The epoxy resins were premixed and stored in syringes at -40°C. The adhesion promoters used were glycidoxypropyltrimethoxysilane (GPS), Bis(trimethoxysilylpropyl) Amine (BTSPA), Bis(triethoxysilane) Ethane (BTSE) purchased from Gelest and used as received, Borosilicate glass (BOROFLOAT) from Erie Scientific Company was used in this study as a substrate for epoxy. The glass was received in the form of 12.7x76.2x0.32 mm slabs. More details of the materials can be found in Chapter 3.

**Table 4.1** Processing parameters of GPS in aqueous solutions to obtain optimum results.

| | **Condition** |
|---|---|
| Silane concentration | 0.5 ~ 2% [11, 15] |
| pH | 4-5 [11, 13, 22] |
| Hydrolysis time | 1 ~ 10 hours [23] |
| Rinsing | Affect film thickness: No rinsing > rinsing in water> rinsing in methanol [12] |
| Drying temperature | Insignificant effect, 93°C ~ 180°C recommended [13, 15,] |

## 4.3 Experimental methods

Double cantilever beam tests were used to obtain the values of critical strain energy release rate of the epoxy/glass interfaces. Locus of failure is detected by using X-ray Photoelectron Spectroscopy (XPS).

### 4.3.1 Double Cantilever Beam (DCB) Specimen Preparation

The DCB testing specimens consisted of sandwiches of glass/Epoxy/glass (glass coated with the experimental adhesion promoter) were prepared. Silane adhesion promoters were diluted to a final concentration of 1 wt% by weight in a solution prepared by 95 wt% methanol and 5 wt% water. First, the surface of glass substrate was cleaned with isopropyl alcohol and treated with ultraviolet/ozone chamber for 20 minute. Then glass substrate was dipped for 2-3 minutes in adhesion promoter solutions, rinsed with methanol, then air dried for 10 minutes. Finally the glass substrate was baked at 110°C for 8 minutes. The resin mixture was placed on the bottom plate, which is along with 250 micron shims. The thermal cured epoxy systems are cured in oven at 60°C for 4 hours then post cure at 150°C for 2 hours.

### 4.3.2 Exposure to hot & humid environment

The DCB specimens were exposed to a hot moisture environment

(85°C and 85%RH) for different periods of time in order to study effect of exposure time in hygrothermal conditions on adhesive strength. The DCB specimens were pre-cracked after aging then tested on Instron. The $G_c$ is reported as a function of aging time. The results are the average Gc of the tested specimens.

### 4.3.3 Adhesion Characterization

DCB tests were conducted using a computer controlled screw driven Instron testing machine (model 5521) in displacement control at a speed of 0.127 mm/min. Tensile force was applied at the end of a specimen in a direction normal to the crack surface which is called cleavage mode (mode II). $G_c$ values, which are in units of $J/m^2$, can be calculated from the following equation [2]: where, P is the applied load, a is the crack length, w is the specimen width (12.7 mm), h is beam height (3.2 mm), and E is the plane strain modulus of glass (62 GPa). $G_C$ can be calculated by Equation 2.5.

### 4.3.4 XPS

Scienta ESCA 300 is used in this research. The take off angle is 90 degrees. Sample size is 0.5in X 0.5in. More details can be found in Chapter 3. All XPS data were obtained with monochromatic Mg Kα radiation and photoelectron takeoff angle of 90°. At this takeoff angle, the sampling depth is about 3.6 nm. Peak identification and compositional analysis based on relative

sensitivity factor calculations were performed by using the casaXPS software version 2.3.12.

## 4.4 Effect of surface treatment on adhesion loss at the interface

To improve the moisture resistance of an adhesively bonded joint, there are several factors to be considered: the surface of the substrate, the nature of the adhesive, the geometries of the bond. First, the surface of the substrate can be modified in many ways to improve the moisture resistance [3, 4, 27].

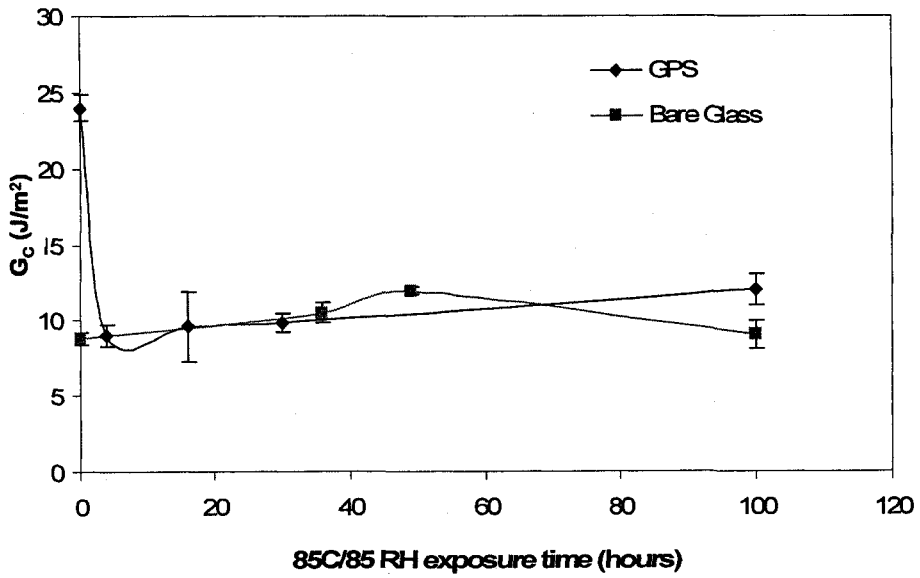


***Figure 4.1*** *Critical strain energy release rates of (a) epoxy and bare glass and (b) epoxy and GPS treated glass.*

Organosilanes have been used for many years to improve adhesion

between polymeric materials and inorganic materials. GPS has an epoxy functional group that can react with curing agent in the model system. They form covalent bonds that can improve adhesion.

Under hot/humid environment, the moisture diffuses into silane/glass interface and breaks the covalent bonds between Silane and glass [4]. Without silane coupling agent, the adhesion between the BisF/EMI epoxy system and glass substrate is 8.8J/$m^2$,

From Figure 4.1 Critical strain energy release rates of (a) epoxy and bare glass and (b) epoxy and GPS treated glass.it can be seen that the surface treatment of 1% GPS silane coupling agent can greatly improve the adhesion at epoxy/glass interface at dry condition from 8.8 J/$m^2$ to 24.0 J/$m^2$. When exposed to 85 °C/85RH, the adhesion drops dramatically. After several hours, the adhesion is almost the same for non-treated and GPS treated glass surfaces. It was also found by other researchers that the principal inconvenience when using silanes is that their chemistry may be influenced by relatively subtle changes in a wide range of parameters [5]. Although the literature in this field is extensive, one major problem remains: the unrepeatability in the experimental conditions chosen by the various workers in this area [12].

When comparing the results by Khayankarn et al. [28] and the above

data, it can be found that the Gc values of GPS treated glass surface are the same, however, the rate of adhesion loss is slightly higher than those reported by Khayankarn et al. The Gc values for the "dry" condition is lower than that reported by Khayankarn. The following factors may have contributed to this difference in adhesion strength.

The spacers used for controlling the bondline thicknesses were glued on the glass surfaces by using superglue in the experiments by Khayankarn et al. However, in this study, the spacers were allowed to stand free between glass plates without using any glue when being used in the above experiments. Using glue to bond the spacers should result in a thicker bondline. In later experiments it can be found that the values of Gc are different with various bondline thicknesses.

Some researchers used dipodal silanes to improve corrosion protection at metal surfaces in harsh environments [3, 56, 26]. Dipodal silanes contain 6 hydrolysable groups at both each ends of the molecular chains. So they can polymerize to form a higher crosslinked structure than regular used silanes with 3-functional groups. Those dipodal silanes, when used alone, to treat the metal surfaces, are found to have a very good corrosion resistance. Also a two-step surface treatment by silane coupling agents was also investigated. GPS and APS are used most often in such tests. The commonly used silane coupling

agents can be used on the top of dipodal treated glass surfaces. The corrosion resistance of the metal surface can also be improved by this means. Song and coworkers tried to use a non-functional dipodal silane (BTSE) with APS to improve corrosion resistance of aluminum. Mixture of silanes can also be used for the same purpose [3]. It turned out that using BTSE alone or BTSE and APS together can improve corrosion resistance of aluminum substrates. The reason above was that BTSE can form a more condensed layer and it is more resistant than APS layer under moisture condition. In addition, amine group in APS is hydrophilic, which makes the ingression of water easier.

APS, GPS, BTSE, BTSPA and combined APS or GPS with dipodal silanes into mixtures at 5:1, 10:1 ratios. A two-step treatment is also investigated, by applying BTSE first, then dip the BTSE treated glass into APS or GPS solutions and follow the same procedure as one-step treatment.

The results are shown in Fig. 4.2. The mixtures of BTSE with APS or GPS do not result in good adhesion, even at dry condition. When used for corrosion resistance, the more highly crosslinked layer has more resistant to moisture ingression. However, for the purpose of promoting adhesion, higher crosslink density means that it is more difficult for the adhesive to interdiffuse into the organosilane layer and form an interphase region. Culler et al, exploring reactions at an interface between an epoxy matrix and a APS silane

film, observed a direct correlation between the extent of reaction and degree of condensation of the APS. They proposed that maximum reactivity at the interface would be achieved when the degree of condensation is smallest, implying that the siloxane layer should not be highly condensed to obtain the optimum performance [31].

From Fig. 4.3, it can be seen that after exposing to 85 °C/85RH for 100 hours, the BTSE/GPS two-step treatment results a higher Gc value than GPS only treatment. Both APS only and BTSPA/APS two-step treated specimens have dropped about 50%. Because BTSPA/APS did not show significantly better performance, and BTSE/GPS would be compatible with UV curable epoxies, which would have more applications in the future, the two-step BTSE/GPS treatment was chosen for further study.

It is expected that the BTSE/GPS two-step treatment doesn't have higher adhesion than GPS treated surface. Based on O. Khayankarn's study, for APS treated glass and BisF/EMI epoxy system, at dry condition, the locus of failure is between APS and epoxy. It is also expected that for two-step treatment, the locus of failure is at the silane/epoxy interface [28].

Time-Gc curve was drawn for BTSE/GPS two step treatment. As shown in Fig. 4.4, the time-Gc curve, although the ultimate adhesion of the

epoxy and glass has no significant difference, moisture ingression was slowed down by application BTSE/GPS adhesion promoters. GPS treated glass has a much greater Gc value at dry condition than bare glass, however, the adhesion drops very fast when exposing to 85°C/85RH conditions.

## 4.5 Epoxy modification

Gc-time curves for filled and unfilled model epoxies are also obtained for GPS treated glass surfaces. The results are shown in Figure 4. 5. Obviously, the fillers in the epoxy matrix help retard the aging process.

Zanni-Deffarges et al. explained one possible reason from the view of shrinkage stresses. When the adhesive bulk is cured, the stress from shrinkage is relatively unconstrained. However, the adhesive in a DCB joint is bond to the adherend, which makes the interfacial region constrained. The shrinkage stress then makes the polymeric material less dense at the interface region, which will be likely to facilitate the ingress of water [32]. So reducing shrinkage stress of the adhesive will make the joints more resistant to water ingress. Adding filler to epoxy matrix can reduce shrinkage during curing procedure. That explains why the adhesion loss of filled model epoxy system is slower than that of unfilled model epoxy system.

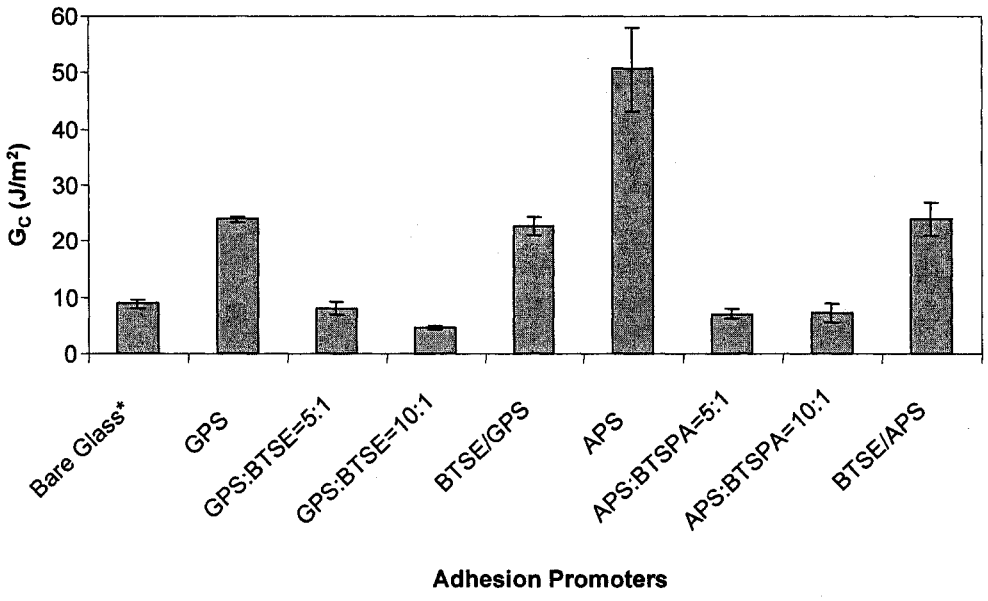


***Figure 4. 2*** *The $G_c$ values of BTSE, BTSPA, APS and GPS treated DCB specimens of Bis F/EMI system.*

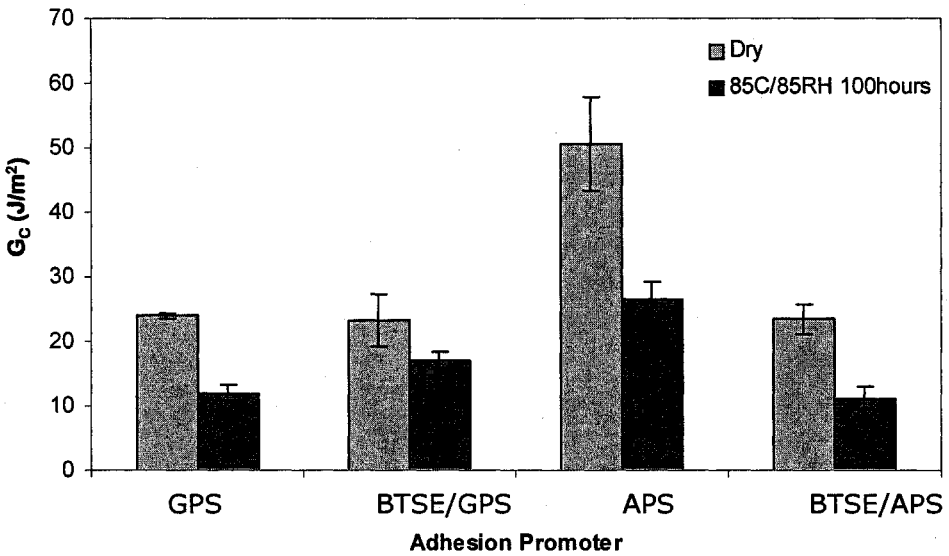


***Figure 4. 3*** *The $G_c$ drop of BTSE, APS and GPS treated DCB specimens under 85°C/85% RH aging condition of Bis F/EMI system.*

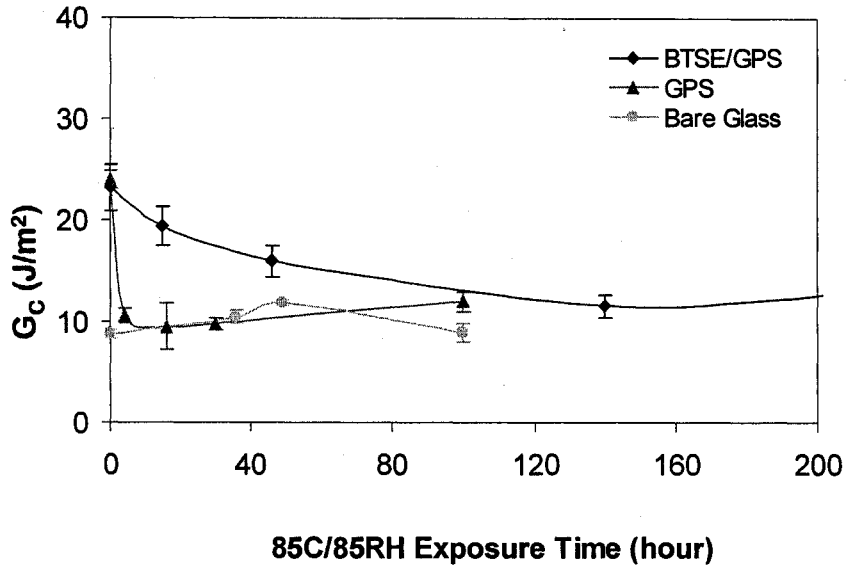


***Figure 4. 4*** *Time-Gc curve for bare glass, GPS treated glass and BTSE/GPS two-step treated glass, with BisF/EMI thermal cure epoxy system, in 85 °C/85RH condition.*

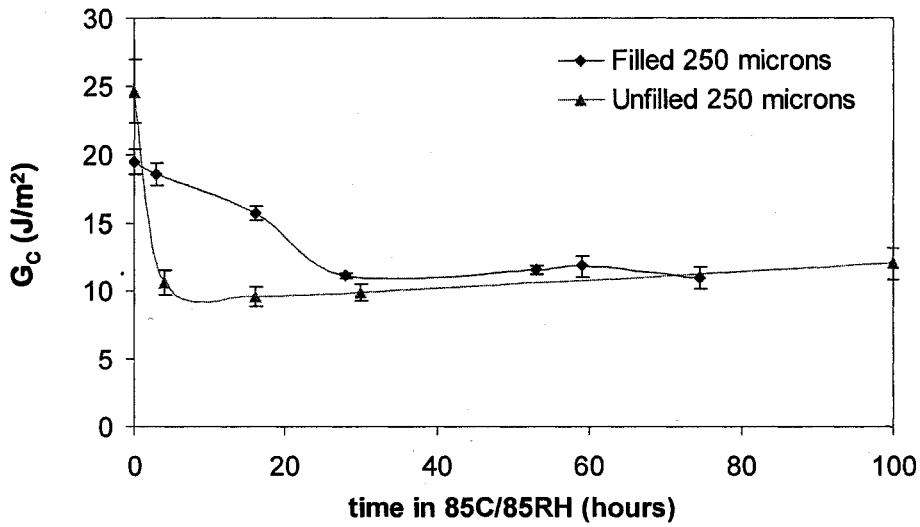


***Figure 4. 5*** *Time-Gc curves for BisF/EMI thermal cured system filled with 40wt% silica and unfilled system, at 85 °C/85RH condition.*

Another factor to be considered is the bonding between fillers and matrix. When water was absorbed into epoxy matrix, it mainly enters the free volume between molecular chains. For filled system, water can also enter the space between fillers and matrix. In this case, the filled epoxy system can work as a desiccater, drying the moisture at the interface, in result, slows down the drop of critical energy release rate at the interface.

## 4.6 Sample geometry on moisture diffusion – effect of bondline thickness

Various bondline thicknesses were used to evaluate the effect of bondline thickness on Gc and moisture ingress. The results are shown in Figure 4. 6. The specimens at 50 microns and 75 microns bondline thicknesses have similar Gc values and the trends are similar too. There is no significant drop of Gc values for these two series of specimens.

Bondline thickness of 250 microns shows very typical Gc-time curve. In which the Gc drops with longer exposure time until reaching a plateau region.

## 4.7 Fracture Surface Characterization by XPS

XPS was used to determine the locus of failure at the neat epoxy/glass

interface in the DCB specimens.

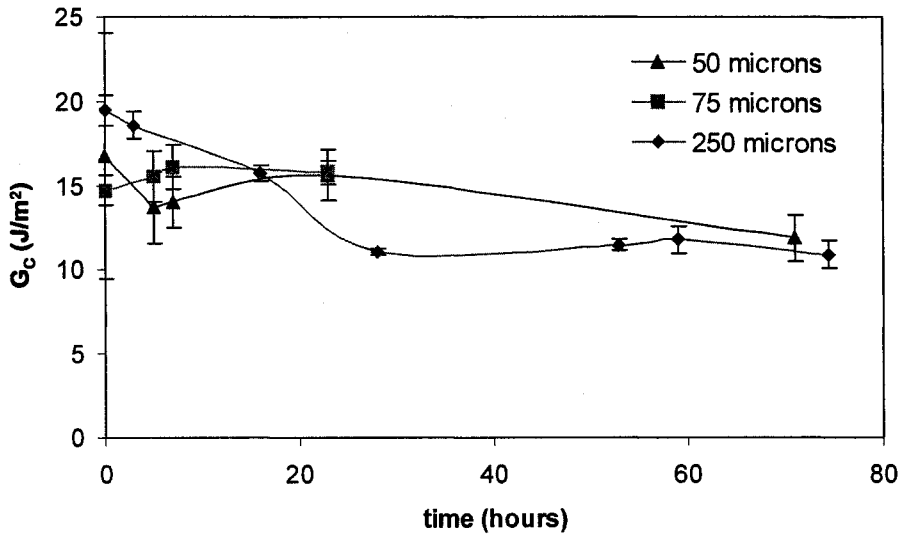


***Figure 4. 6*** *Time-Gc curves for BisF/EMI thermal cured epoxy system (filled with 40% silica) at different bondline thickness at 85 °C/85RH condition.*

Fig. 4.7 shows XPS survey scans of the fracture surfaces. The peaks of C (285 eV), O (530 eV) and Si (100 eV) were used to analyze the composition of the fracture surfaces. Fig. 4.8 compares the ratios of Oxygen to Carbon and Silicon to Carbon at the fracture surfaces for DCB samples at dry/wet conditions respectively. The ratio of O/C of pristine epoxy fracture surface is

0.2. The sample of GPS treated glass plate, which has an O/C ratio of 4.1, was used to represent the composition of GPS layer. From

Figure *4.*(a), it shows that. O/C at the surface of epoxy at 0 day is 0.2. This value is the same of pristine epoxy surface; on the glass side of the same DCB sample, O/C is 0.5. This value is quite close to the value of pristine epoxy, and much less than the GPS coated glass, which is 4.1. So the composition of this fracture surface is mainly epoxy, with very little GPS content. From these results, we can conclude that the specimen has cohesive failure. The fracture surfaces are within the epoxy layer.

After 9 days of exposure at 85 °C/85RH, the O/C at epoxy side of the DCB sample is still 0.2, which suggests that the fracture surface is at the epoxy side. However, the O/C ratio on the glass side of the same DCB sample is 7.5. This value is higher than BTSE/GPS treated glass, and lower than BTSE coated glass. This value suggests that the fracture surface at the glass side should be the silane layer. The value of the fracture surface at 9 days is in between the values of the two silane treated glass surfaces, which also proves that there interdiffusion of GPS into BTSE layer. From these values we can conclude that the fracture surface is between the silane (GPS) and epoxy phases. After 9 days, the failure mode is adhesive failure. From Fig. 4.8(b) we can draw the same conclusion.

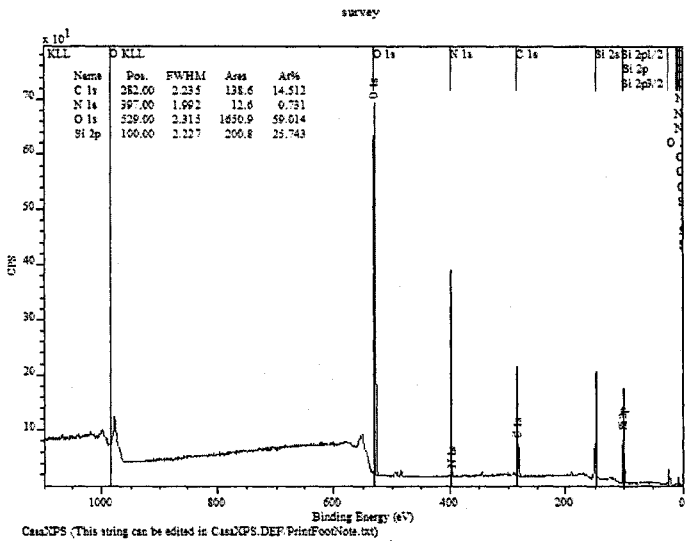


(a)

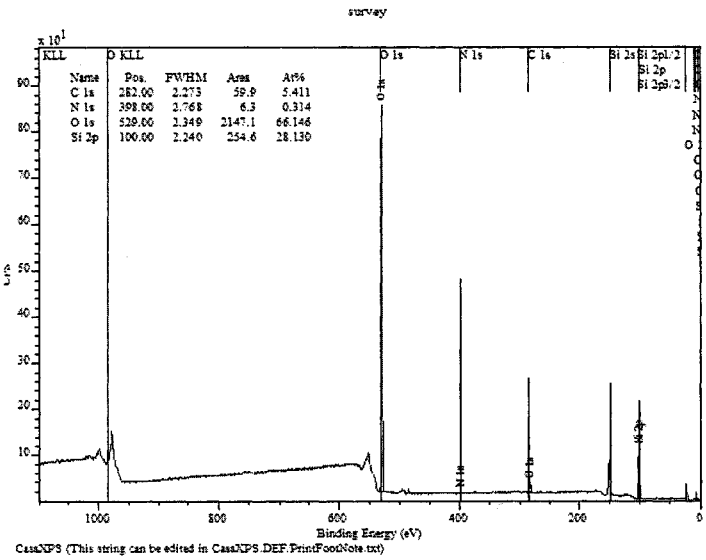


(b)

***Figure 4.7*** *XPS survey scans of fracture surfaces of DCB samples: (a) GPS treated glass surface; (b) BTSE/GPS treated glass surface;*

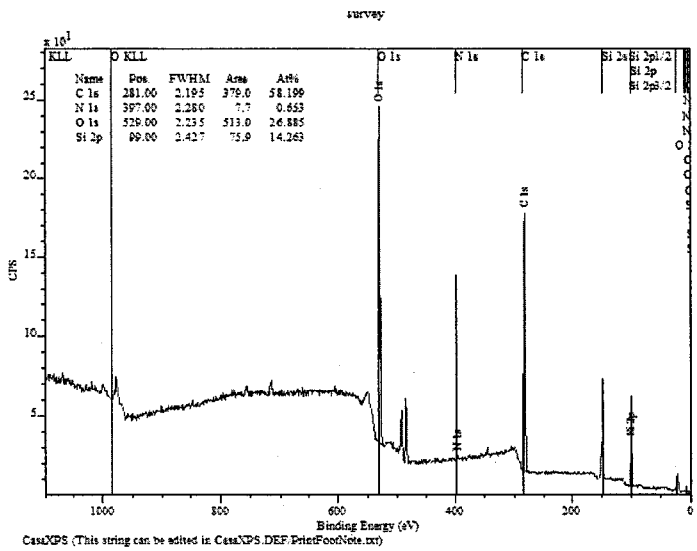


( c)

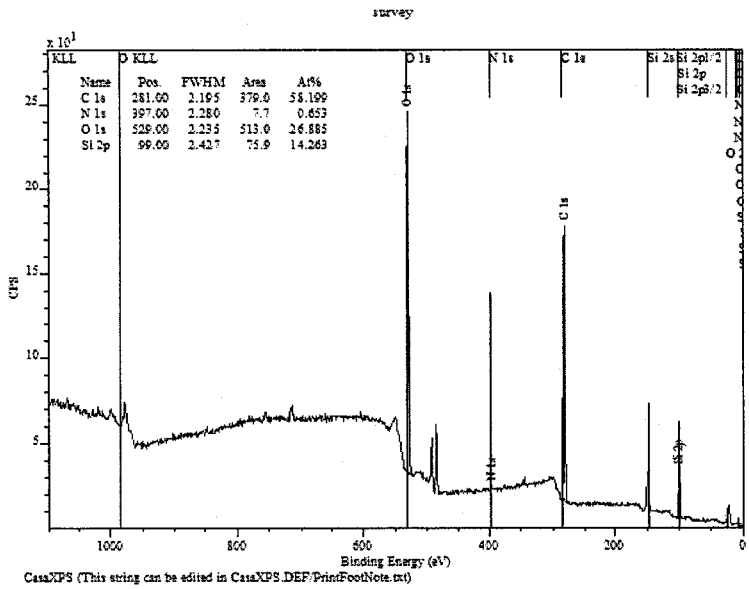


(d)

***Figure 4.7*** *XPS survey scans of fracture surfaces of DCB samples:* (c) BTSE/GPS two-step treated DCB samples dry: glass side; (d) BTSE/GPS two-step treated DCB samples 9 days in 85 °C/85RH: glass side;

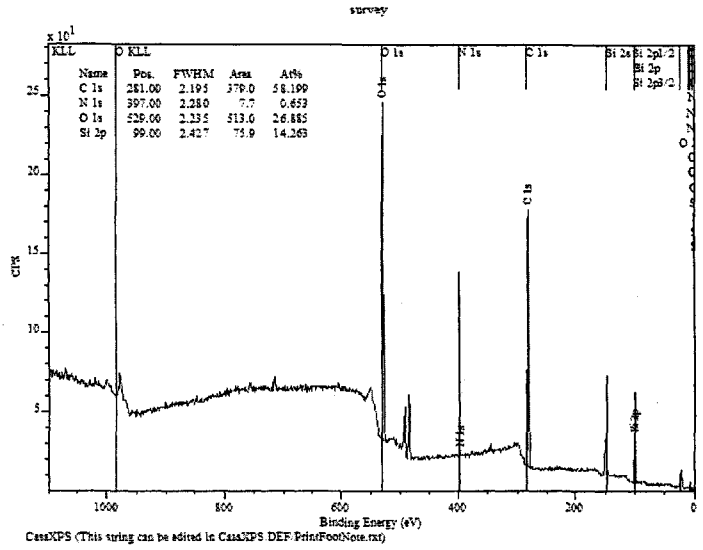


(e)

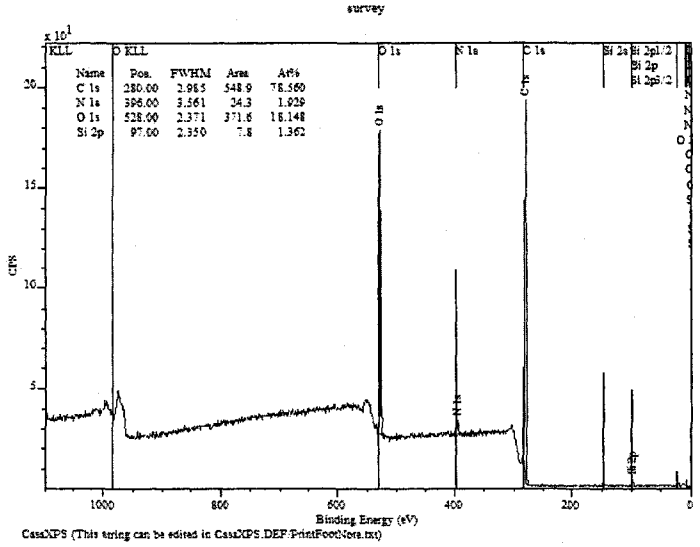


(f)

***Fig. 4.7*** *(e) BTSE/GPS two-step treated DCB samples dry: epoxy side; (f) BTSE/GPS two-step treated DCB samples 9 days in 85 °C/85RH: epoxy side*

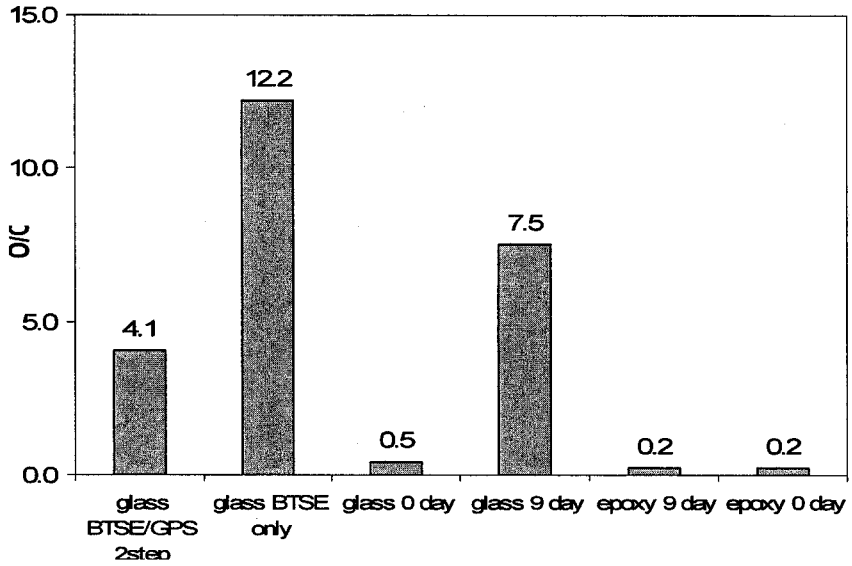


(a)

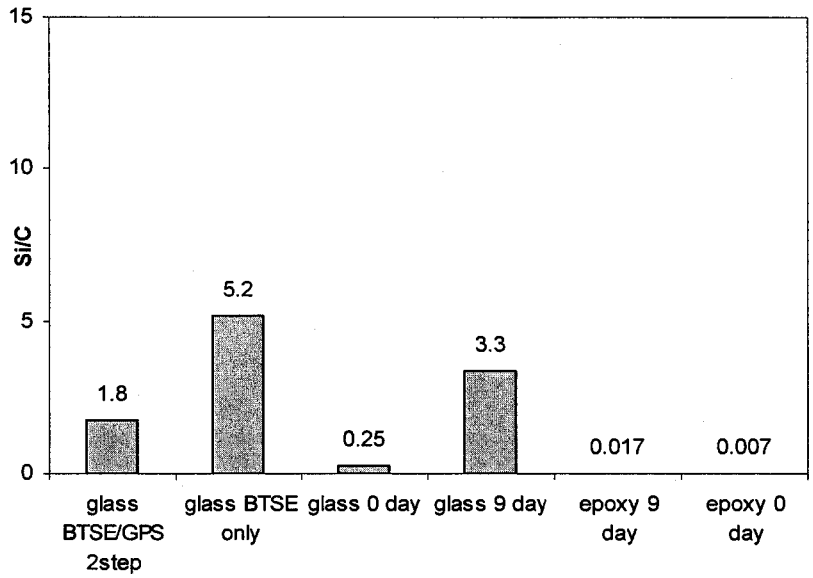


(b)

***Figure 4.8*** *Ratios of (a) O/C and (b) Si/C at the fracture surfaces of both epoxy and BTSE/GPS treated glass sides for the dry condition and 9 days in 85 °C/85RH.*

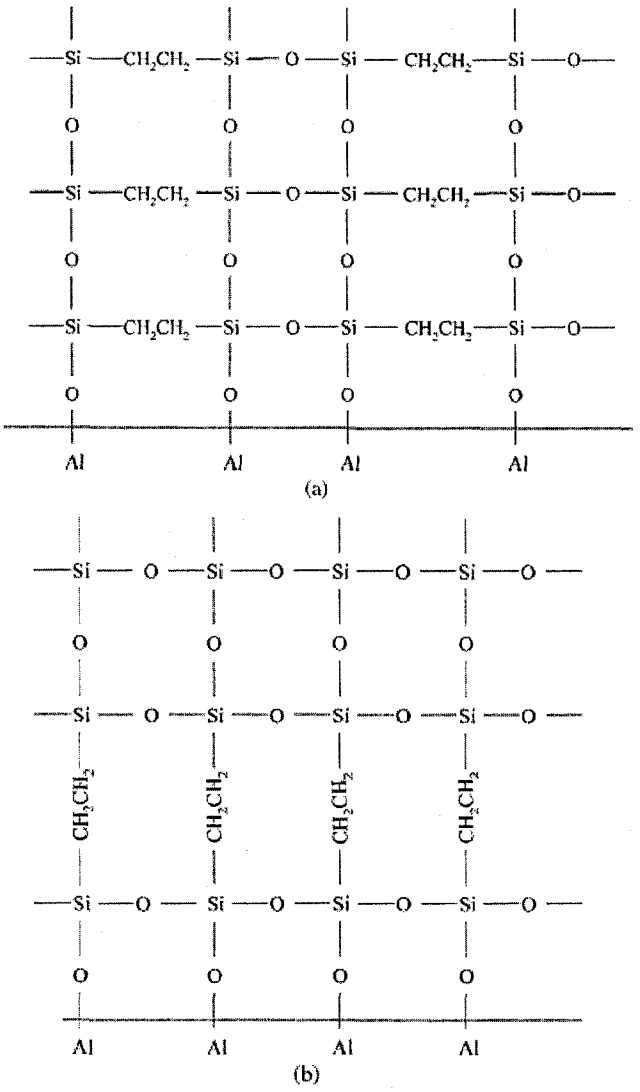


***Figure 4.9*** *(a) Schematic of adsorption of BTSE on aluminum showing non-porous film. (b) Another schematic of adsorption of BTSE on aluminum showing non-porous film [3].*

There are two pristine samples. BTSE/GPS two-step treated glass surface has a Si/C ratio at 1.8. BTSE treated glass has a Si/C ratio at 5.2. Since the BTSE forms a denser and more compact thin film at the glass surfaces, there are more silicon elements at the top surface, as seen in Fig. 4.9 [3].

The Si/C ratio at the pristine epoxy side should be 0.

At 0 day of 85 °C/85RH, the Si/C is 0.0065 at the epoxy side and 0.25 at the glass side. Those values are close to the values of pristine epoxy. It indicates the same conclusion as (a) that the specimen has cohesive failure. The fracture surface is at the epoxy bulk. Please note that the values are not 0 because there is interdiffusion between epoxy, GPS and BTSE. Some of the silicon element close to the surface could be detected.

After 9 days in 85°C/85RH, the Si/C ratio of epoxy side of the DCB sample is 0.017, which is still quite low. This value indicates that the composition of the fracture surface is mainly epoxy. On the other side of the sample, the Si/C ratio is 3.3. This value is in between of the GPS and BTSE. The debonding path is between epoxy and silane layer. The failure mode is adhesive failure after 85 °C/85RH for 9 days.

## 4.8 Conclusions

1. A Two-step treatment of BTSE/GPS can improve the moisture

resistance for a model system epoxy BisF/EMI over that of bare glass and GPS treated glass.

2. A mixture of dipodal and GPS or APS do not improve adhesion presumably due to higher crosslink density in the silane layer.
3. Adding in fillers can slow down moisture ingression in DCB specimens
4. Bondline thickness ranges from 50 microns to 250 microns, did not show significant effect on adhesion and moisture resistance, comparing with surface treatment or adding fillers to matrix.
5. The failure mode of epoxy with BTSE/GPS two-step treated glass plates changes before and after exposing to 85°C/85RH humidity. The failure mode was cohesive failure when the specimen was dry, and failure happened within epoxy bulk. After exposing to 85°C/85RH for 9 days, the failure mode changed to adhesive failure.

## 4.9 References


1. T. C. Wong, L. J. Broutman, Polymer Eng Sci, 25(9), 529, (1985).
2. B. Blackman, J. P. Dear, A. J. Kinloch, and S. Osiyemi, Journal of Materials Science Letter, 10: p. 253, (1991).

3. J. Song, W. J. van Ooij, Journal of Adhesion Science and Technology, Volume 17, Number 16, pp. 2191-2221(31) (2003).

4. E. P. Plueddemann, Silane Coupling Agents, New York: Plenum Press (1982).

5. M. L. Abel, J. F. Watts, R. P. Digby, The Journal of Adhesion, 80: 291-312, (2004).

6. K. L. Mittal, (Ed), Silanes and other coupling agents, VSP: the nehterlands; (1992).

7. S. J. Shaw, In: Ellis B, (Ed). Chemistry and technology of epoxy resins. London: Blackie; (1993).

8. C. L. Olsson-Jacques, A. R. Wilson, A. N. Rider, D. R. Arnott, Surf Int Anal 24:569 (1996).

9. A. N. Rider, D. R. Arnott, Surf Int Anal 24:583, (1996).

10. A. N. Rider, D. R. Arnott, Int J Adhes Adhes 18:261 (1998).

11. M. L. Abel, R. D. Allington, R. P. Digby, N. Porritt, S. J. Shaw, Watts, J. F., International Journal of adhesion & adhesives, 26, 2-15, (2006).

12. M. L. Abel, J. F. Watts, R. P. Digby, International Journal of Adhesion and Adhsives 18, 179-192 (1998).

13. M. L. Abel, J. F. Watts, R. P. Digby, The Journal of adhesion 80: 291-312, (2004).

14. G. Tesoro, Y. J. Wu. Adhes. Sci. Tchnol. 5:771 (1991).

15. N. H. Sumg, A. Kaul, I. Chin, C. S. P. Sung, Polym. Eng. Sci. 22:637,

(1982).

16. F.D. Osterholtz, E. R. Pohl, J. Adhes. Sci. Technol. 6, 127, (1992).
17. H. Ishida. Polym Compos 5, 101, (1984).
18. D. E. Leyden, J. B. Atwater, J Adhes. 24, 145, (1988).
19. A. A. Baker, R. J. Chester, Int. J. Adhes. Adhes. 12, 73 (1992).
20. R. A. Gledhill, S. J. Shaw, D. A. Tod, Int. J. Adhes. Adhes. 10, 192, (1990).
21. R. P. Digby and S. J. Shaw, Int. J. Adhes. Adhes. 18, 261-264, (1998).
22. F. D. Osterholtz, E. R. Pohl, Kinetics of the hydrolysis and condensation of organofunctional alkoxysilanes: a review. Journal of Adhesion science and Technology. 6(1), 127-49, (1992).
23. M. L. Abel, M. M. Chehimi, A. M. Brown, S. R. Leadly, J. F. Watts, Spectra. New York, (1996).
24. C. M Bertolsen, F. J. Boerio, Journal of adhesion, vol 70, 259-279, (1999).
25. B. G.. Tilset, A. Bjorgum, F. Lapiqu. F., Simensen, C. J., Proceedings of the Annual meeting of the Adhesion Society 25$^{th}$, 177-179, (2002).
26. B. G.. Tilset, F. Lapique, A. Bjorgum, C. J. Simenen, Proceedings of the international symposium on silanes and other coupling agents, June 11-13, (2004).
27. W. J. van Ooij, Sabata A., Surf. Interface. Anal. 20, 475 (1993).
28. O. Khayankarn, Ph.D. dissertation, Lehigh University, Bethlehem, PA,

USA (2004).

29. R. J. Kuhbander and J. J. Mazza, SAMPE Synp. 38, 1225-1234 (1993).
30. N. Porrit, Ph.D Dissertation, University of Surrey, Surrey, UK, (2001).
31. S. R. Culler, H. Ishida, J. L. Koenig, J col Interf Sci 109:1, (1986).
32. M. P. Zanni-Deffarges, and M. E. R. Shanahan, International Journal Adhesion and Adhesives, 15: 137 (1995).

# CHAPTER 5

# MODELING ADHESION LOSS IN DCB SPECIMENS

---

The adhesion of UV cured epoxy (NSC G3PS1) system with borosilicate glass was tested. It was found that the $G_c$ values of the DCB specimens can be modeled by a "composite" assumption based on the area of the "wet" and "dry" parts in the specimens. The tested values of $G_c$ are compared with the calculated values. SEM pictures of the fracture surfaces were taken.

## 5.1 Background

### 5.1.1 Moisture diffusion into adhesive bonded joints.

OLED and PLED technologies have attracted a great interest in recent years. They have the advantages of efficient electroluminescence at low voltage, high contrast in dark room and lower overall costs [1]. The greatest

concern about OLED and PLED is their relatively short operation life time, which limits their application. Besides the possibility of internal degradation [2,3,4], water and oxygen may dramatically reduce the life time of organic devices [5, 6]. Therefore, OLED or PLED are packaged in an inert atmosphere to prevent the device from being exposed to moisture and oxygen. One packaging solution is to apply glass on top of the LED device and seal the glass with an adhesive.

Epoxy resins are widely used as matrices for adhesives, coatings, sealants, packaging materials and structural composite materials due to their outstanding adhesive-bonding properties [8, 9, 10, 11]. Since its first recognition in 1944, adhesives have been formulated to meet various specifications and use criteria and become the most valuable use for epoxy resins. The advances in UV-cured epoxy in recent years, such as low cost, low curing temperature, space saving equipments, short production time, makes them candidates for sealing on OLED/PLED devices. Although epoxy can be used as sealant to keep OLED from harsh environment, moisture diffusion rate through epoxy sealant is still relatively fast comparing with OLED's expecting life-span for electronic application. Epoxy resins normally have weakened properties by the pick-up of water in a hot/humid environment [12, 13]. So their utilization at elevated temperature or humid environment has been limited by their thermal stability. Fig. 5.1 shows that the hot/wet tropical environment

was by far the more hostile and that the presence of an applied load increased the rate of loss of strength [14]. The strength of the joints after aging in a hot/wet tropical location is obviously lower than those in a hot/dry environment.

Therefore, two properties of epoxy adhesive should be considered as sealants for OLED/PLED displays. First, it should maintain good adhesion to substrate when exposing to hot/humid environment; second, the diffusion rate of water in the joint should be as low as possible. The behavior of the epoxy/substrate interface under severe environment is very important for improving moisture and oxygen resistance, which further more, will improve the life span of OLED and PLED.

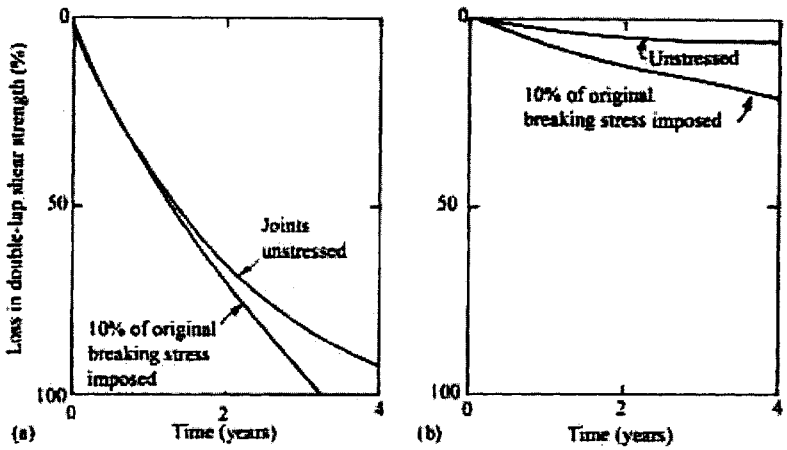


***Figure 5. 1*** *Effect of outdoor weathering on the strength of epoxy-polyamide/aluminum alloy (chromic-acid etched pretreatment) structural joints [14]. (a) Hot/wet tropical site (b) Hot/Dry desert site*

The goal of this work is to provide insight into the hygrothermal aging of epoxy/glass interfaces. It is anticipate that such insights could be used to improve modeling of existing adhesive systems as well as develop new surface treatment methods which help epoxy/glass interfaces gain excellent long term durability under hygrothermal condition and fulfill industry requirements. The purpose of this work is to study the behavior of moisture diffusion at epoxy/inorganic material interfaces in order to predict loss of strength of adhesive joints in hygrothermal environment.

There are many theories addressing adhesion between

polymer/inorganic interfaces, including wetting and spreading [15] boundary-layer theory [16], surface-attachment theory of adhesive joint strengths [17], and much more [18] Fowkes et al. [19] explained the adhesion of polymer to inorganic oxides in terms of acid-base interactions between the acidic or basic surface sites. These interactions are strong under dry conditions but the strength of adhesion drops dramatically after hygrothermal aging. By this theory, forming primary chemical bonds by using silane coupling agents can improve the adhesion between substrate and adhesive [20, 21, 22].

### 5.1.2 Capillary diffusion through adhesive/substrate interfaces

The method that is most often used to study moisture diffusion in epoxy adhesives is the gravimetric method. However, it was found that diffusion behaviors are quite different between interface and bulk phase. Shanahann et al. studied the moisture diffusion behavior and proposed a "capillary diffusion" theory [15]. For this reason, the weight gain measurements can not reflect the adhesion loss at the interfaces although it can provide some information on moisture uptake in the bulk. Shanahan used a "composite" model to explain water ingression in epoxy bulk.

Kent et al. [23] used neutron reflectivity and angle-resolved XPS to examine the adsorption of water at silicon/polymer interfaces. By silane diffusing to the interface and promoting adhesion, a sharp reduction in the

amount of water at the interface was found.

There are many references investigating loss of adhesion under hot humid environment. However, most of them assume the interface in the studied joints were uniform in adhesion. In our experiments, it was found when using the NSC G3PS1 as studied material, the epoxy system changes color when absorbing water. Very clearly there is a transition between center and edge parts in the specimens. Here we try to use a "composite" model to analyze the water ingression in the DCB joints.

## 5.2 Materials

An experiment, UV-cured epoxy-based adhesive NSC G3PS#1 from National Starch & Chemicals, Inc. was bonded to Borosilicate glass (BOROFLOAT) from Erie Scientific Company. The glass was received in the form of 12.7x76.2x0.32 mm slabs. The one-part adhesive was supplied in syringes.

## 5.3 Experimental methods

### 5.3.1 Adhesion testing using Double Cantilever Beams (DCB)

The simplest fracture mechanics specimen to generate and analyze is the uniform double cantilever beam specimen [24]. This specimen is shown in

Fig. 5.2 and described in ASTM D3433.

The DCB testing specimens consisted of sandwiches of glass/Epoxy/glass were prepared. The resin mixture was placed on the bottom plate, which is along with spacer materials to control the bondline thickness. One glass plate was placed on the top and the specimens were then cured under a 400 W metal halide UV lamp which yield an intensity of 35 $mW/cm^2$. The specimens are cured for 4 minutes each side.

The DCB specimens were exposed to moisture at 85°C/85%RH for different periods of time in order to study effect of aging time on adhesive strength. The DCB specimens were cracked after aging. The $G_c$ values are reported as a function of aging time.

Adhesion testing was performed using a computer controlled screw driven Instron testing machine in displacement control at a speed of 0.127 mm/min. Tensile force was applied at the end of a specimen in a direction normal to the crack surface which is called cleavage mode. $G_c$ values, which are in units of $J/m^2$, can be calculated from the following equation by Equation 2.5, where, P is the applied load, a is the crack length, w is the specimen width (12.7 mm), h is beam height (3.2 mm), and E is the plane strain modulus of glass (62 GPa).

$$G_c = \frac{12P^2a^2}{w^2h^3E} \qquad \text{(Equation 2.5)}$$

As the load was applied, the crack propagates, the crosshead is reversed to unloaded further then reloaded subsequently. This cycle was repeated in order to get several $G_C$ values for averaging. $G_C$ values can be determined from the load-displacement plot shown in the following figure.

### 5.3.2 Scanning Electron Microscopy SEM

JEOL 6300 Scanning Electron Microscope was used to examine the fracture surface of the DCB specimens. The fractured DCB samples were cut into 25.4mm X 12.7mm X 3.2mm shapes and sputter coated with a thin layer of gold-palladium on the fracture surfaces. SEM images are obtained with accelerating voltage of 3 kV.

## 5.4 Modeling $G_C$ assuming a "composite structure"

### 5.4.1 $G_C$-time curve for NSC G3PS1 adhesive

The Gc-time curve was obtained as shown in Fig. 5.3, the lines were by least square fit. It can be noticed that for both bondline thicknesses, the rates of $G_c$ loss are very similar. The slope for the one at 250-micron bondline is -0.13

and the one for 125-mircon bondline is -0.14. As loss of $G_C$ reflects the adhesion property at the interface of the joint, those numbers showed that the rates of loss of the $G_c$ are about the same. In another word, the moisture update at the interface is about the same, although the bondline thicknesses are different.

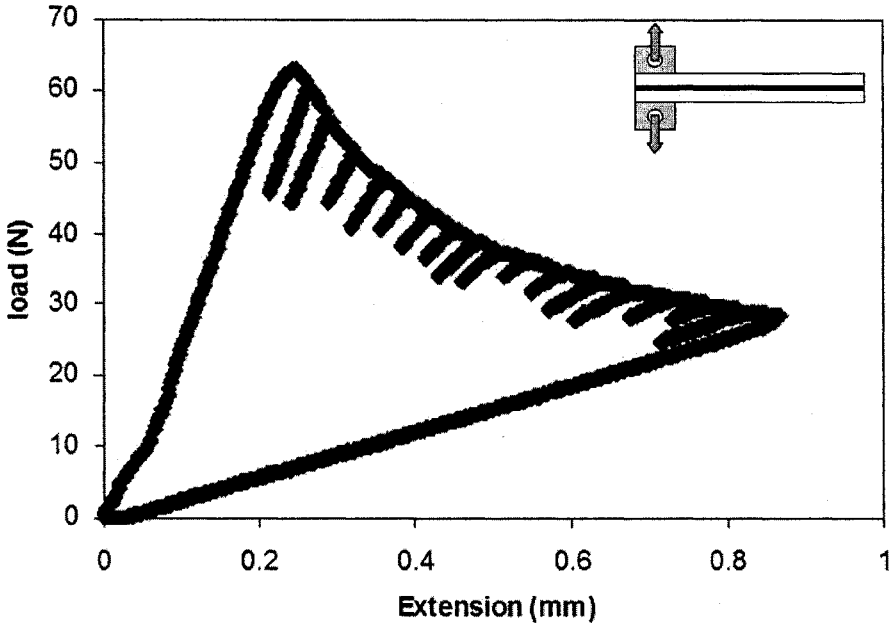


***Figure 5.2*** *Diagram of the data obtained from the DCB test*

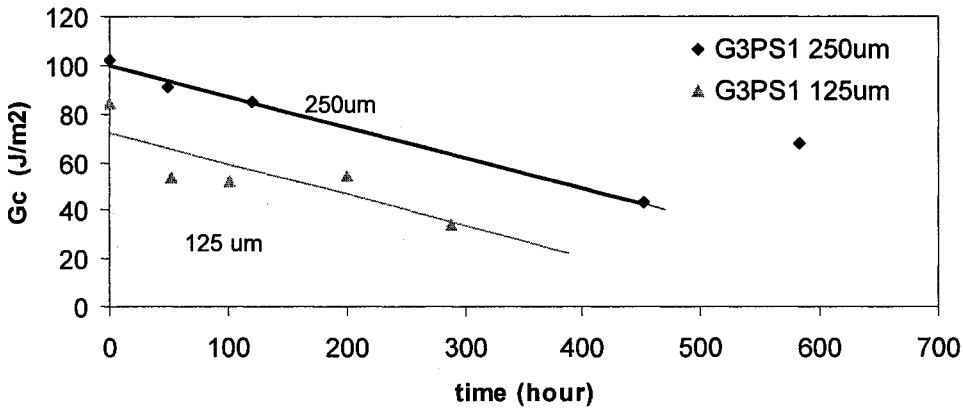


***Figure 5.3*** *$G_c$-time of NSC PS1 of 250-micron and 125-micron bondline thicknesses*

An important observation of this sealant is that as the moisture diffuses in, the color of the sealant changes from brown into yellow. Fig. 5.4 shows the color change of a DCB sample at different exposing time to 85°C/85RH. From this color change, it is easy to evaluate where the moisture diffusion front is before further testing such as INSTRON or failure mode determination.

Moreever, the color change (location of the front line of the yellow color) were found to be directly related with the DCB testing results. At the fracture surfaces, it is very obvious that in the area of brown color, which is at the center region, the failure mode is cohesive failure; in the areas of yellowish color, which are closer to the edge, the failure mode is adhesive failure. The center region, which dark brown in color, is getting smaller and smaller. Fig. 5.5 showed the correlation of the $G_C$ values with the width of the area of adhesive and adhesive failure. When the whole specimen has adhesive failure, the specimen can be easily broken apart. The Gc is very low at this point, so it is assumed to be zero.

Fig. 5.6 is the schematic drawing of the water diffusion into a DCB specimen. As described in (a), water diffuses in from the interface region first, then from the interface, where water concentration is higher than the bulk phase, water diffuses into bulk phase. In (b), the cross section drawing shows that when water diffuses into the interface, color of the adhesive starts to

change, as can be seen from Fig. 5.4. Because the interface picks up water before the bulk, the color change starts from the interface, as we can see in fig. 5.6 (b). That explains why from the top view of the DCB specimens, there is a region with lighter yellowish color between the "dry" and "wet" regions.

***Figure 5.4*** *Color of DCB specimens at different exposing time to 85°C/85RH*

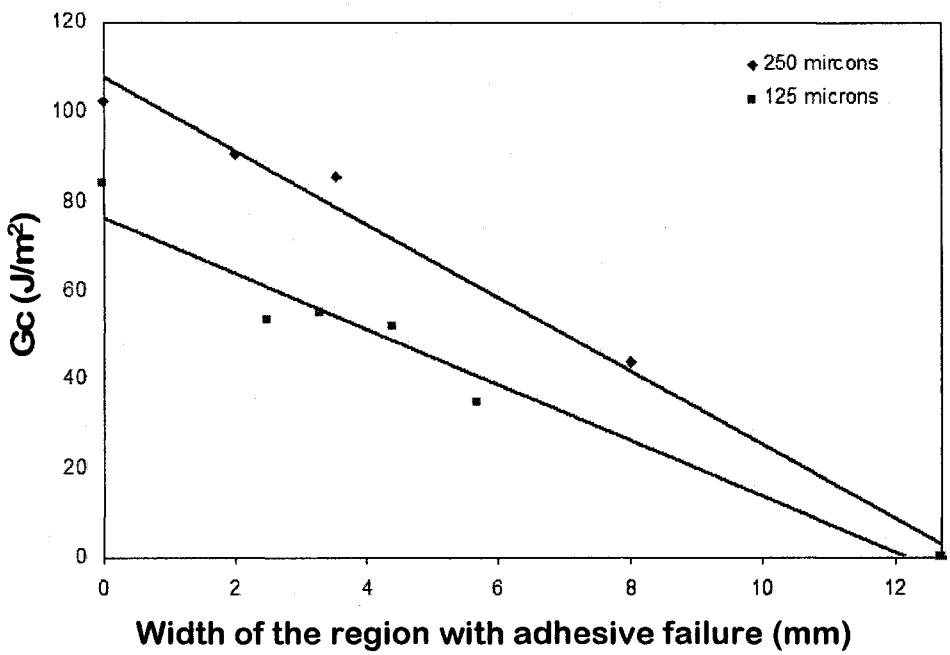


***Figure 5.5*** *Correlation of $G_C$ with the width of the area with adhesive failure for both 250 microns and 125 microns bondline thicknesses.*

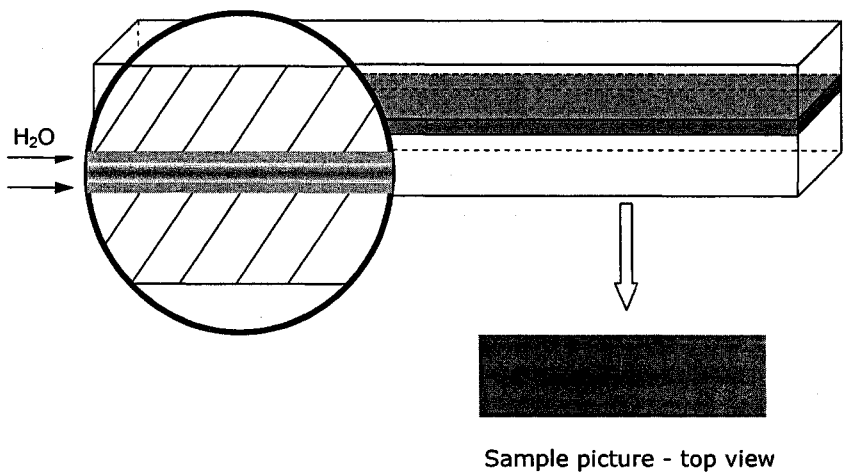


(a)

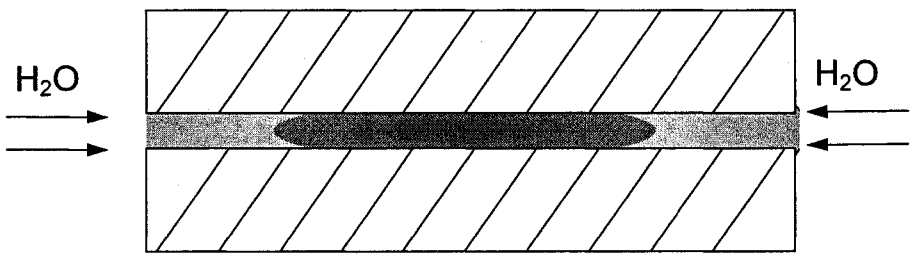


(b)

***Figure 5. 6*** *The schematic drawing of the DCB specimen with water diffusion into the interfaces. (a) the side view (b) cross section of the DCB specimen.*

In a study by Wu and coworkers [32], higher water concentration at the interface than in bulk was detected. Using Neutron Scanning experiment, excess water was discovered within 30Å of the silicon/polymer interface, where the water concentration reached 17% (by volume) for the samples without a coupling agent and 12% for the ones with coupling agent. Beyond the interface, the water concentration was measured at 2 to 3%, which is typical of bulk polyimide [18, 32,].

For the DCB specimens, the interface is the key role that determines adhesion. As more water is absorbed at the interface than the bulk, the changes in adhesion are greater than the changes in bulk properties. In weigh gain tests on DCB specimens, the information obtained is mainly from the bulk because the interface region is so thin. From the study by Khayankarn et al., the strain energy release rate for DCB specimens was found to drop to the lowest value while at the same time moisture pickup of the specimen is still increasing (Fig. 5.7) [25]

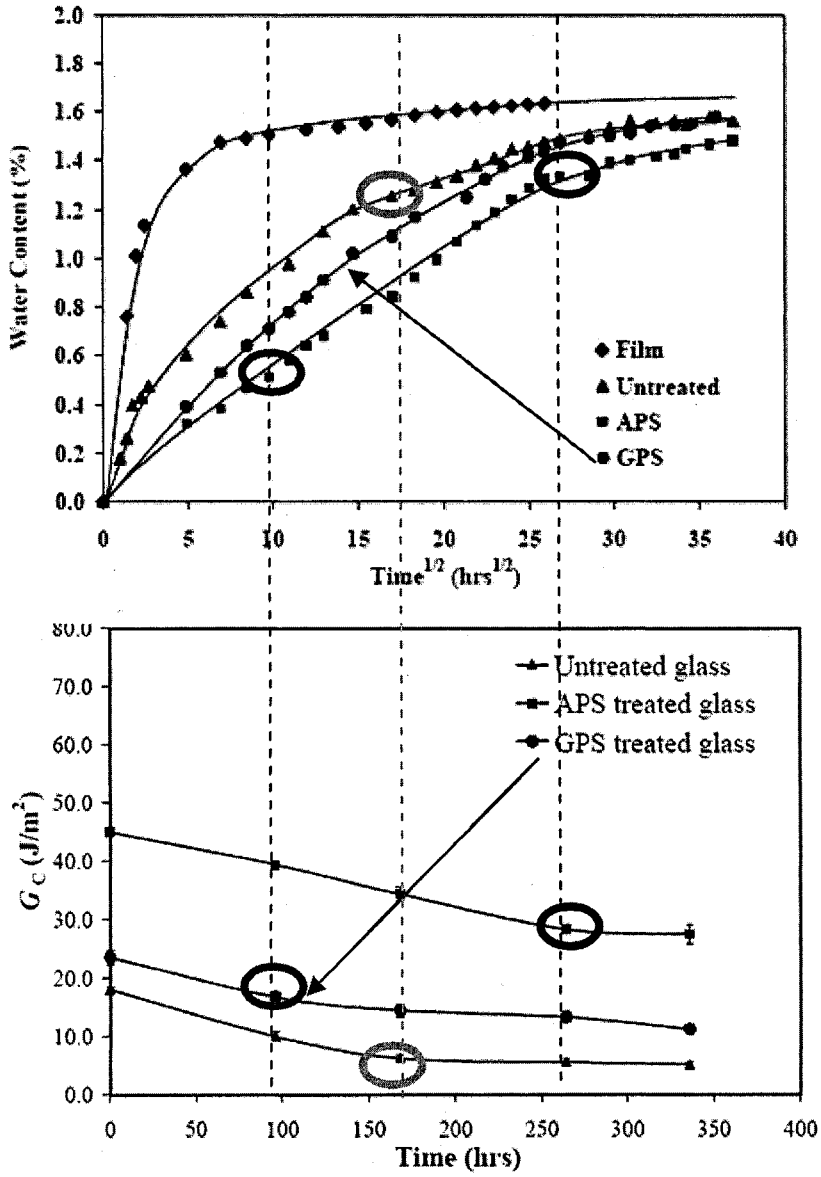


***Figure 5.*** *7 (a) Weight gain of DCB specimen for thermal cured BisF/EMI model system with stand free film, untreated glass surfaces, APS and GPS treated glass surfaces when exposed to 85°C/85RH condition;(b) Gc drop of untreated glass surfaces, APS and GPS treated glass surfaces when exposed to 85°C/85RH condition [25].*

For a DCB specimen, when calculating the average strain energy release rate for a DCB specimen, the assumption is the interface is uniform. However, when moisture diffuses into the adhesive joint, the moisture enters the joint from the edge at the interface first. We can easily find this out from our DCB samples tested. At the areas closer to the edge, the adhesive and the substrate easily delaminates, and the crack tip propagates before the crack tip at the center region at the specimen. So if we separate the "wet" and "dry" areas and calculate the Gc, we may get more information from our results, or even calculate Gc based on fracture surface without doing DCB tests.

Assumptions for the modeling:

- Front line of absorbed water is sharp
- The adhesion in "dry" and "wet" areas is uniform, respectively.

Based on the parameters that relate to Gc calculation (Equation 2.5), one can get :

$$G_{c\text{-}comp}^{1/2} = x\, G_{c\text{-}dry}^{1/2} + (1\text{-}x)\, G_{c\text{-}wet}^{1/2} \qquad \text{(Equation 5.1)}$$

Where $G_{c\text{-}comp}$ is the overall Gc for the whole specimen, $G_{c\text{-}dry}$ is the Gc for the center region, where we assume is still dry, and the $G_{c\text{-}wet}$ is the Gc for the areas closer to the edge, where water has already diffused into. As described in Fig. 5.4 from the NSC PS1 adhesive, we can clearly see the color

change at these two regions.

### 5.4.2 Comparison between calculated Gc and tested Gc.

Table 5.1 shows the calculated and tested Gc values. From Fig. 5.8 we can see the comparison more clearly, the calculated values and tested results are quite close.

Fig 5.9 and 5.10 show the fracture surfaces of DCB samples at difference locations. The sample width is 12.7 mm. X values in Fig.5.10 is the distance to the left edge of the sample.

**Table. 5.1** Comparison between calculated Gc and tested Gc.

| Sample #* | $W_1$(wet) (mm) | $W_2$(dry) (mm) | $G_c$ (dry) ($J/m^2$) | $G_c$ (tested) ($J/m^2$) | $G_c$ (calculated) ($J/m^2$) | time (hours) |
|---|---|---|---|---|---|---|
| 1 | 0 | 12.7 | 102.4 | 102.4 | 102.4 | 0 |
| 1 | 1.8 | 10.9 | 102.4 | 90.7 | 87.9 | 49 |
| 1 | 2 | 10.7 | 102.4 | 85.5 | 86.3 | 121 |
| 1 | 7.5 | 5.2 | 102.4 | 43 | 41.9 | 451 |
| 2 | 0 | 12.7 | 84.5 | 84 | 84.5 | 0 |
| 2 | 2.5 | 10.2 | 84.5 | 53.3 | 67.9 | 52.5 |
| 2 | 4.4 | 8.3 | 84.5 | 52 | 55.2 | 101 |
| 2 | 3.3 | 9.4 | 84.5 | 54.7 | 62.5 | 200 |
| 2 | 5.7 | 7 | 84.5 | 34.5 | 46.6 | 250 |

*sample #1 is with bondline thickness is 250um, and sample #2 is with 125 microns bondline thicknesses.

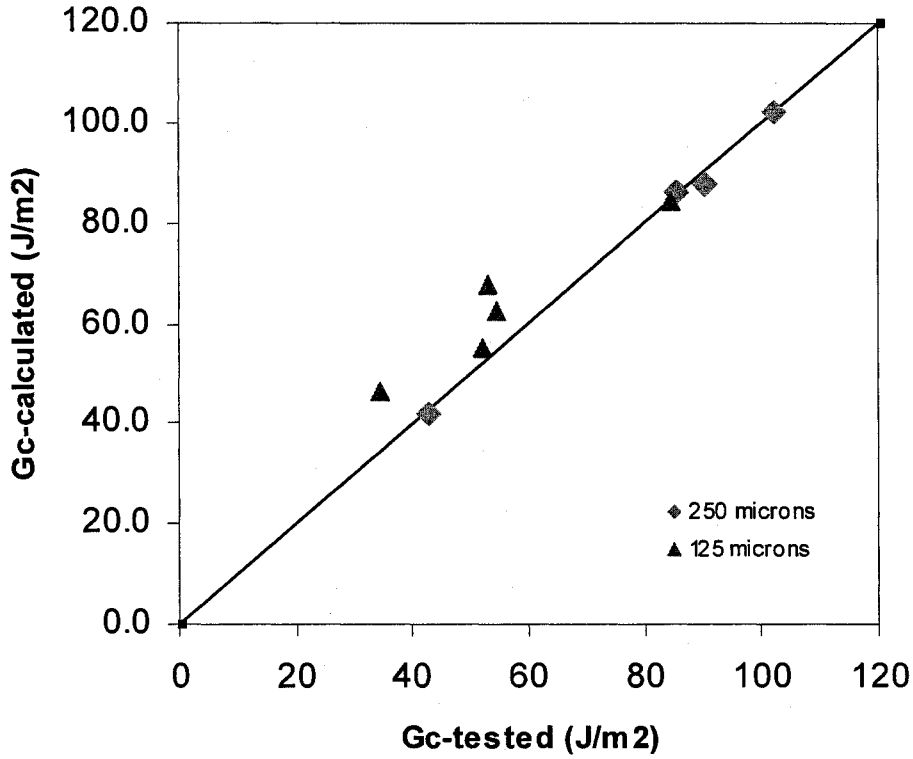


***Figure 5. 8*** *Comparison of calculated and tested Gc values.*

### 5.4.3 SEM Images for Fracture Surfaces

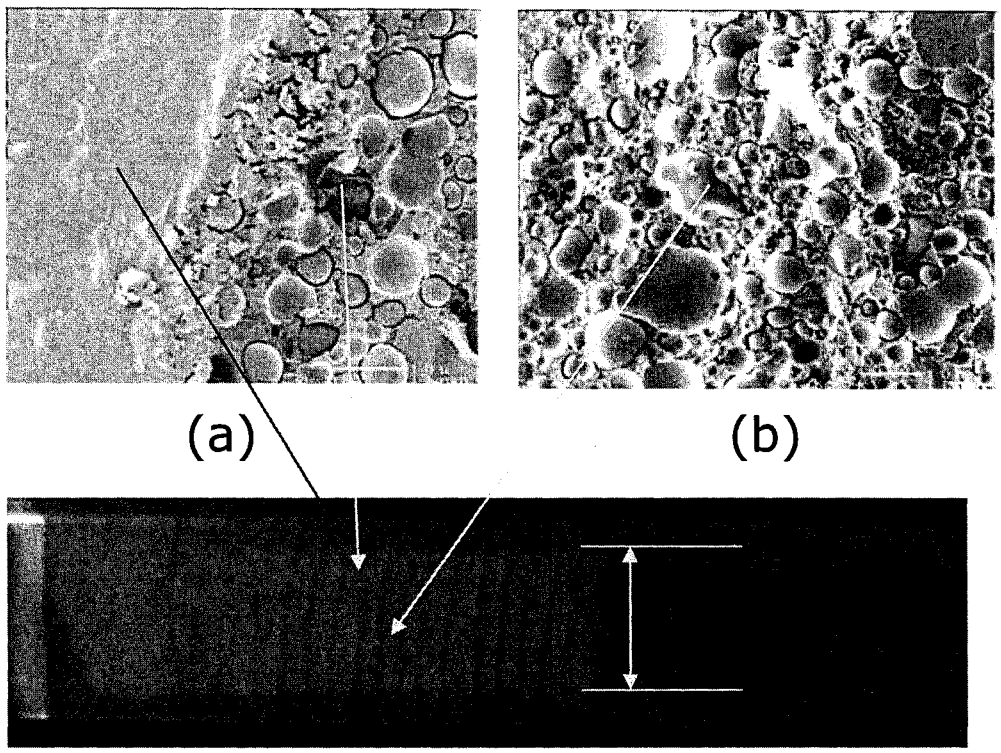


***Figure 5. 9*** *SEM images of DCB specimens at the fracture surfaces. (a) both adhesive and cohesive failure (b) cohesive failure*

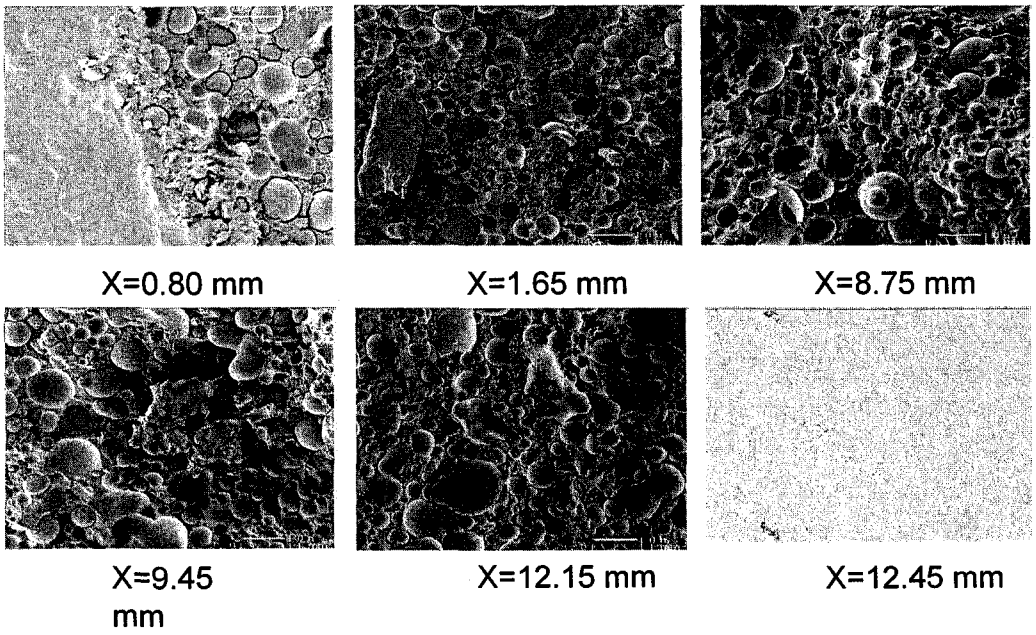


***Figure 5. 10*** *SEM images of DCB specimens at the fracture surfaces at different locations.*

### 5.4.4 Diffusion coefficient

Diffusion coefficient is an important parameter to evaluate a material's ability for water permeation. When calculating diffusion coefficient, the most common method is weight gain test. The diffusion coefficient of NSC G3PS1 was tested by Y. Chuang [33], the diffusion coefficient of NSC G3PS1 bulk adhesive is $2.6x10^{-8}$ $cm^2/s$. If the diffusion coefficient is the same at the interface and bulk, then the water would diffuse into the adhesives would be far less than 1 cm for over 500 hours exposure at 85°C/85RH. From the color change, which is due to the absorption of water, and the Gc drop of the samples, we can know this is not the real case. This suggests that diffusion coefficient is a lot higher at the interface for this adhesive joint.

## 5.5 Conclusions

For the DCB samples consisting of NSC G3PS1 bonded between two glass slabs, there is clear color difference between the areas at the center regions and the areas closer to the edge. The calculated Gc values and tested values of NSC G3PS1 are very close. SEM images of the fracture surfaces of aged DCB specimens show two distinct regions: a cohesive failure region and an adhesive failure region that is smooth. Therefore a model for adhesion loss was developed based on the size of both regions. This composites model works

well for the NSC G3PS1 epoxy system. Calculated Gc based on the width of the area of cohesive failure and adhesive failure. This model should be applicable to other adhesive systems where there are distinct differences between wet and dry adhesion.

The model suggests that adhesion loss can be retarded by reducing the rate of capillary diffusion of moisture.

## 5.6 References


1. C. W. Tang and S. A. Van Slyke, Appl. Phys. Lett. 51, 913, (1987).
2. E. M. Han, L. M. Do, N. Yamamoto and M. Fujihira, Thin Solid Films, 273, 202, (1996).
3. H. Aziz. And G. J. Xu, J. Phys. Chem. B 101, 4009, (1997).
4. B. H. Cumpston and K. F. Jensen, Synth. Met. 73, 195, (1995).
5. D. Kolosov, D. S. English, V. Bulovic, P. F. Barbara, S. R. Forrest and M. E. Thompson, J. Appl. Phys. 90 3242, (2001).
6. Y. Liew, H. Aziz, N. Hu, H. S. Chan, G. Xu and Z. Popvic, Appl. Phys. Lett. 77 2650, (2000).
7. M. S. Xu, J. B. Xu , H. Z. Chen and M. J. Wang, J. Phys. D: Appl. Phys. 37, 2618, (2004).
8. H. Lee and K. Neville, Handbook of Epoxy Resins, New York, McGraw Hill, (1967).
9. P. F. Briuns, Epoxy Resin Technology, New York: Interscience Publishers,

(1968).

10. L. Nicodemo, F. Bellucci, A. Marcone and T. Monetta, Journal of Membrane Science, 52, 393, (1990).
11. W. J. Schultz, International Encyclopedia of Composites, Vol. 2, ed. S.M. Lee. New York: VCH Publishers, (1990).
12. E. L. McKague, J. D. Reynolds and J. E. Halkias, Journal of Applied Polymer Science, 22, 394, (1978).
13. P. S. Theocaris, E. A. Kontou and G. C. Papanocolaou, Colloid and Polymer Science, 261, 394, (1983).
14. J. L. Cotter, W. C. Wake (Ed), *Developments in Adhesives*, 1. Applied Science Publishers, London, (1977).
15. M. P. Zanni-Deffarges. And M. E. R. Shanahan, Int. J. Adhesion and Adhesives 15 137-142, (1995).
16. H. E. Garrett, Aspects of Adhesion, 2, 18, (1964).
17. A. F. Lewis and R. T. Natarajan, Adhesion science and technology (L.H. Lee, ed.), Plenum Press, New York, 98, 563, (1975).
18. C. A. May, Epoxy Resins: chemistry and technology, 2nd ed. New York, (1968).
19. F. M. Fowkes, D. W. Dwight, D. A. Cole, J. Non-Cryst. Solids 120, 47, (1990).
20. D. Hunston, K. Macturk, C. Schultheisz, G. Holmes, W. McDonough, C. L. Schutte, EURADH 96, Cambridge, 1996, Vol. 1, London: The Institute

of Materials, 427-432, (1996).

21. C. L. Schutte, W. McDonough, M. Shioya, M. McAuliffe, M. Greenwood, Composites 25, 617, (1994).
22. E. P. Pleuddemann, J. Adhesion, 2, 184, (1970).
23. M. S. Kent, G. S. Smith, S. M. Baker, A. Nyitray, J. Browning, G. Moore, and D. W. Hua, J. of Mat. Sci. 31, 927, (1996).
24. A. V. Pocius, Adhesion and Adhesive Technology, Hanser Publishers, (1997).
25. O. Khayankarn, Ph.D. Dissertation, Lehigh University, Bethlehem, PA, USA, (2004).
26. A. J. Kinloch, Adhesion and Adhesives: Science and Technology, Chapman and Hall, London, (1987).
27. B. Blackman, J. P. Dear, A. J. Kinloch and S. J. Osiyemi, Mat. Sci. Lett. 10, 253, (1991).
28. J. Crivello, Chem. Mater. 9, 1554, (1997).
29. W. J. van Ooij, J. Adhes. Sci. Tech. 11, 29, (1997).
30. W. J. van Ooij, Chemtech., 28, 26, (1998).
31. R. I. A. Toniolo, Hiimmelgen, Macromol. Mater and Eng, 289, 311, (2004).
32. W. Wu, W. J. Orts, C. J. Majkrzak, H. Water, L. Donald, Polymer Eng. and Sci., 35, (12), 1000, (1995).
33. Y. Chuang, Mater Thesis, Lehigh University, Bethlehem, PA (2005).

# CHAPTER 6

# SUMMARY AND CONCLUSIONS

## 6.1 Summary

### 6.1.1 Adhesion loss in a model epoxy system

The adhesive strength of BisF/EMI model epoxy systems was investigated. Several factors that could affect the adhesive strength of the joints were evaluated to get a better understanding of adhesion loss of adhesive joints under hygrothermal conditions.

The first factor studied was the surface treatment of the substrate. The glass plate was coated by silane coupling agents. Previous research in this group had found that the surface treatment by APS and GPS could improve moisture resistance of the joints under hygrothermal conditions [1,2], and they had better improvements than most of the other silane coupling agents tested. In this study, APS and GPS based coatings are modified with dipodal silanes. Two coating procedures were used: 1) a monosilane and dipodal mixture, or 2)

dipodal-then-monosilane two-step process.

It was found that the mixture of dipodal silane coupling agent and monosilane resulted in poor adhesion between epoxy and glass substrate. Four formulations were tested: BTSE:GPS at 1:5, BTSE:GPS at 1:10, BTSPA:APS at 1:5, BTSPA:APS at 1:10. All of them resulted in poor adhesion. For these silanes, only Gc at dry conditions were tested, because the adhesion strength is already quite low. Since the dipodal silane molecule each has six -OR groups, while the APS or GPS only have three -OR groups in each molecule, the resulting crosslink density of the films from the mixtures of silanes are higher than that of films formed by using monosilanes [3]. The higher crosslink density of the silane film would make it more difficult for the epoxy system to diffuse into, and results in a weaker interphase region.

Note that BTSE does not have functional groups that can react with epoxy systems. When BTSE is mixed with monosilane to coat the glass surface, the density of the functional group (Amino group of APS, or epoxy group of GPS) at the surface of the film would be diluted by BTSE molecule because the –OH groups in BTSE molecules could also stay on the top layer of the silane film. This would reduce the number of the chemical bonds formed between silane film and epoxy systems. This observation is in agreement with the results seen in the corrosion resistance test by Song et al. [4] They found

that for polyurethane paint on top of silane treated aluminum, the trend of corrosion protection from good to bad is: two-step BTSE/APS, BTSE only, mixture of BTSE and APS, APS only. For polyester paint on top of silane treated aluminum, the trend is: two-step BTSE/APS, mixture of BTSE and APS, BTSE only, APS only. The reason is that BTSE is compatible only with polyurethane paint so the use of BTSE can provide good corrosion protection; on the other hand, BTSE is not compatible with polyester paint. So the corrosion protection is not as good as mixture of BTSE and APS, in which APS can react with polyester coating. This is very similar to our case. The mixture of BTSE and GPS has a reduced density of epoxy functional group at the surface of the silane film, which results in a weaker interphase region. So the adhesion is lower than BTSE/GPS two-step treatment or GPS only treatment.

For BTSPA, there is a functional group (-NH-) that is able to react with epoxy systems. However, this secondary amino group is in the middle of the dipodal molecule. After the –OH groups at both sides form a crosslinked network with the dipodal itself and the monosilane, the –NH- group will be highly restrained in the network instead of staying on the surface. So the epoxy system will be less likely to reach a –NH- group and react with it. BTSPA also has six –OR groups so the crosslink density of the mixture with monosilanes should be also higher than that of a monosilane. So again, it will be more

difficult for the epoxy system to diffuse into the silane film. And the result is a weaker interphase region.

For the two-step treatment, BTSE and GPS are selected for the investigation. Because the screening tests of BTSPA and APS have comparable performance with BTSE plus GPS. BTSE and GPS were chosen for a more in depth study since they are compatible with UV cured epoxy systems (do not interfere with UV curing reaction).

The two-step treatment of BTSE/GPS offers better moisture resistance for the model epoxy systems than bare glass surface or GPS treated glass surface. The rate of adhesion loss of those adhesive joints is slower than GPS treated surface or bare glass. However, for a longer time, when the adhesion drops to a plateau region, the adhesive joint by two-step treatment does not show significantly better adhesion than GPS treated surface or the bare glass surface. So in a short term exposure to 85°C/85RH, the adhesion loss is slowed down by the two-step treatment than GPS treated surface. This agrees with the study by Song et al. in their corrosion resistance tests that their two-step treatment by BTSE/APS offered better corrosion resistance than BTSE alone, mixture of BTSE and APS, or APS alone [4]. In a long term exposure, finally the adhesion strength falls into comparable level with GPS. This observation is in agreement with similar tests done by Kinloch [5]. They used two-step

treatment by BTSE/GPS to coat aluminum surface then tested $G_c$ and $G_{th}$. Their conclusion was that the two-step treatment by BTSE/GPS didn't offer better adhesion under dry or wet conditions, either for critical or subcritical strain energy release rate. However, from our Gc-time curve, we can see that at in fact they could be referring to specific conditions. There are two regions in this Gc-time curve. At the beginning, the Gc was decreasing with exposure time (region I). After a certain time, Gc reaches to a plateau region, then Gc doesn't drop with extension of exposure time (region II). In our tests, BTSE/GPS two-step treatment takes much longer time than GPS only one-step treatment to reach the plateau region. In region I, BTSE/GPS two-step shows better moisture resistance than GPS treatment for the same exposure time. After they both reach region II, the values of critical energy release rate for both treatments are quite close. At this point, if the adhesion strength of each treatment is compared, it will be found that the two treatments have similar adhesion strength.

Other than surface treating the glass substrate by silane coupling agent, there are other factors we evaluated for the DCB adhesive joints.

One is the nature of epoxy system. Narsavage-Heald et al. have investigated the effects of adding silanes to epoxy bulk to improve adhesion and moisture resistance. In this current project, we tried to use epoxy system

filled with silica particles and compared it with unfilled epoxy systems. It was found that the adhesion loss of filled system is slower than unfilled system.

In Shanahan's paper on 'capillary diffusion', he explained one possible reason for the capillary diffusion is it could be related to the effects of shrinkage stresses. When the adhesive bulk shrinks during cure, the stress is relatively unconstrained. However, in an adhesive joint, the interracial region will be constrained by adherend. This could lead to effective dilation of the polymeric material in the vicinity and a less dense structure, possibly facilitating the ingress of water and leading to a higher local average diffusion coefficient. [6]. Adding fillers to epoxy systems is a very common method to adjust or control the shrinkage of the epoxy. This is a plausible explanation why our filled system has better moisture resistance than unfilled system.

In practical application of epoxy adhesive, the bondline thickness is a factor that possibly affects the moisture diffusion. We have evaluated several bondline thicknesses but no meaningful tread was found in those cases.

### 6.1.2 Adhesion loss in a commercial UV-cured adhesive

We also proposed a model to predict adhesion loss based on the area of cohesive failure and adhesive failure on a commercial UV cured epoxy. The predicted values of adhesion by the model fit well with the experimental data.

The assumptions of the model are:

- The change from "wet" area to "dry" area is abrupt
- Within the "wet" or "dry" area, Gc is uniform

SEM images were taken to evaluate assumption 1. The images clearly showed abrupt changes from adhesive failure to cohesive failure.

## 6.2 Conclusions

- In our study, it was found that a two-step treatment of BTSE/GPS on the surface of glass substrate can improve the moisture resistance for a model system of thermal cured epoxy Bis F/EMI when compared to a bare glass surface and a GPS treated glass surface.
- The treatment of the surface of the glass substrate by a mixture of dipodal and monosilane cannot improve adhesion at dry condition presumably due to higher crosslink density at the interphase region.
- The adhesion loss of filled model epoxy system is slower than unfilled model epoxy system.
- For the BTSE/GPS two-step treated specimens, the failure mode is cohesive failure before exposing to 85C/85RH humidity; the fracture surface is within the epoxy bulk. After exposing to 85C/85RH humidity for

9 days, the failure mode is adhesive failure and on the glass side, the fracture surface is at the GPS/BTSE interphase.

- The commercial UV-cured adhesive exhibited a clear difference between the areas at the center regions and the areas closer to the edge. The calculated Gc values by our proposed model and tested values are very close.
- The SEM images for the fracture surfaces of the DCB specimens show there is no noticeable difference within the area with cohesive failure or adhesive failure, respectfully. The surface of the area with adhesive failure is uniform and smooth.

## 6.3 References


1. D. Narsavage-Heald, and R. A. Pearson. Proceeding 24th Annual Meeting of The Adhesion Soc. (2001).
2. O. Khayankarn, Ph.D. Dissertation, Lehigh University, Bethlehem, PA, USA (2004).
3. H. Yim, M. S. Kent, J. S. Hall, J. J. Benkoski, E. J. Kramer, J. Phys. Chem. B, 106, 2474-2481, (2002).
4. J. Song, W. J. van Ooij, J. Adhesion Sci. Technol. Vol. 17, No.16 pp.2191 (2003).
5. A. N. N. Adams, A. J. Kinloch, R. P. Digby, S. J. Shaw; Adhesion

99, International Conference on Adhesion and Adhesives, 7th, Cambridge, United Kingdom, Sept. 15-17, 205-210, (1999).

6. M. P. Zanni-Deffarges, and M. E. R. Shanahan, International Journal Adhesion and Adhesives, 15: p. 137, (1995).

# CHAPTER 7

# SUGGESTIONS FOR FUTURE WORK

---

The following research is suggested for future work:

- Test hygrothermal aging of different model systems and commercial available sealants, different surface treatments, and validate the model on these systems and use it to calculate the interfacial diffusion coefficient and bulk diffusion coefficient, then study the interfacial diffusion and bulk diffusion separately, and give a guideline for product formulation
- Use the model as a guideline for depositing OLED sealant, and determining the minimum width of the bond needed for the required lifetime of the device.
- Predict the time needed for moisture passing through the adhesive joints, relate adhesion loss at different hygrothermal conditions, and obtain master curves for the time needed for moisture passing through the interface at different humidity or temperature, which will help decide the width of the bond of adhesives.

# Vita

Xiaohan Zhang was born in February, 1975 in Tianjin, China, to Mr. Guoning Zhang and Ms. Xiuzhi Dong. In 1993, she went to Chemical Engineering Department in Tsinghua University, Beijing. In 1998, she received Bachelor Degree in Chemical Engineering. She was admitted by the Polymer Science and Engineering Program of Lehigh University under the supervision of Prof. Raymond A. Pearson in 2000. In Jan. 2007, she got a M.S. degree on the study of crack initiation and propagation of epoxy bulk and epoxy/aluminum interfaces. She completed her research project on the study of adhesion loss at epoxy/glass interfaces under hygrothermal conditions and received her Ph. D. degree in Jan. 2007. She received Graduate Student Merit Award from Lehigh University in 2004.